This document was prepared in conjunction with work accomplished under Contract No. DE-AC09-76SR00001 with the U.S. Department of Energy.

DISCLAIMER

OSR 24-A116
(REV 9-80)

E. I. DU PONT DE NEMOURS & COMPANY
INCORPORATED
ATOMIC ENERGY DIVISION
SAVANNAH RIVER LABORATORY
AIKEN, SOUTH CAROLINA 29808
(TWX: 810-771-2670, TEL: 803-725-6211, WU: AUGUSTA, GA.)

DPST-83-529-TL

CC: R. Maher, SRP
E. B. Sheldon
S. Mirshak, SRL
SRL Record Copy (4)

June 22, 1983

Acc. No. 10322

J. T. GRANAGHAN, PLANT MANAGER
SAVANNAH RIVER PLANT

ATTENTION: D. C. NICHOLS (30)

TIS FILE
RECORD COPY

COMPUTER MODELING OF SALTSTONE LANDFILLS
BY
INTERA ENVIRONMENTAL CONSULTANTS

Ref: "Parametric Modeling for Design of a Waste Disposal Facility." Report from Intera Environmental Consultants to E. I. Du Pont. December 31, 1982. (Attached)

The referenced report describes the computer modeling studies performed for SRL by Intera Environmental Consultants. These modeling studies were used to improve saltstone landfill designs and are the basis for the current reference design. The modeling studies and how the results of these studies were used to estimate contaminant releases to the groundwater, are summarized in the attached report (DPST-83-529). With the reference landfill design, EPA Drinking Water Standards can be met for all chemicals and radionuclides contained in SRP waste salts.

Intera is currently doing further modeling work for SRL to determine if the wider saltstone trenches, proposed by the Engineering Department, significantly changes contaminant release rates. They are also calculating the distance needed to achieve thorough mixing of salts into the groundwater beneath the saltstone landfill. This will determine how far the landfill boundary (fence) is placed from the saltstone trenches.

E. L. Albenesius

E. L. Albenesius, Research Manager
Waste Disposal Technology Division

MDD:ske
Disc 2

DPST-83-529

TECHNICAL DIVISION
SAVANNAH RIVER LABORATORY

CC: W. R. Stevens, III
T. V. Crawford
P. L. Roggenkamp
I. W. Marine
W. R. McDonnell
W. G. Holmes
C. M. King
H. W. Bledsoe
J. R. Cook
H. C. Wolf
SRL Record Copy (4)

ACC. NO. 103221

June 17, 1983

TO: E. L. ALBENESIUS

FROM: M. D. DUKES (2)

TIS FILE
RECORD COPY

COMPUTER MODELING OF SALTSTONE LANDFILLS
BY
INTERA ENVIRONMENTAL CONSULTANTS

INTRODUCTION AND SUMMARY

During the past year Intera Environmental Consultants, Inc. of Houston, Texas has worked closely with SRL to computer model a variety of potential landfill designs for the disposal of saltstone in the unsaturated zone.[1]

With the improved landfill designs and a new low permeability saltstone developed at SRL, a new reference salt disposal system has been chosen. This system consists of low permeability saltstone blocks covered with a clay cap. Computer modeling shows that this system will permit groundwater to meet EPA drinking water standards[2] for all chemicals and radionuclides in saltstone.* The evolution of the new reference disposal system is traced in this report.

---

* SRL has worked on the assumption that if drinking water standards are met for nitrate and nitrite all other chemicals and radionuclides will be within standards. This imposes the most severe restrictions based on current regulations.

The Model

A saturated-unsaturated finite element computer code of groundwater flow was used to evaluate the various landfill designs. The computations were two-dimensional and were based on cross-sections taken perpendicular to the trenches (Figure 1). Landfills were evaluated at steady-state flow assuming continuous infiltration of water at a rate of 15 inches per year. There are small variations in the water flux at depth during extended wet or dry periods. However, to insure that these variations do not significantly effect the predicted release rates or the water quality downflow of the burial area transient cases (varying moisture flux) will be modeled by Intera in future studies.

Unsaturated hydraulic conductivity data used for soil, clay, and saltstone were average curves for these types of materials since specific data were not available. Future studies will include calculations using actual unsaturated hydraulic conductivity values for the specific materials. Little change in salt release is expected with these refined calculations. Saturated hydraulic conductivity data were supplied to Intera from SRL studies (Table 1).

The most important information that Intera provides to SRL from the model is the fraction of the total recharge (percolating rainwater) that flows through the saltstone blocks. Laboratory experiments have shown that water flowing through saltstone comes out saturated with salts. The composition of this saturated salt solution is shown in Table 2. It is assumed, for making estimates of contaminant release from saltstone, that any water flowing through a saltstone block exits with this salt content (53,600 ppm N) and that this solution is then diluted by the water which has been diverted around the saltstone block.

Nitrogen releases in this report are calculated as follows:

$$\text{ppm N in saturated solution} \times \frac{\text{recharge water passing through saltstone}}{\text{total recharge water}}$$

$$= (53600 \text{ ppm N}) \times \text{fraction of recharge through saltstone}$$

The Original Saltstone Landfill (Cases A and B)

The first saltstone landfill modeled by Intera was the original reference disposal system containing eight

20' x 20' x 250' blocks surrounded by a large continuous clay cap and clay liner with permeabilities of 10^{-7} cm/sec (Table 1). For simplification, half of the symmetrical system was modeled (Figure 2).

Assuming that the landfill is in place with material properties shown in Table 1 (Case A), it takes 12-13 years before steady-state flow is reached. At steady-state, water was perched on top of the clay cap in this system as high as 8-10 ft in the center. This perched water and the degree of saturation throughout Case A are shown in Figure 3.

The flow of water through this system is depicted in Figure 4, which shows that approximately 20% of the recharge water flows through the clay encased landfill. This is because of the width of the clay cap (110 ft) and the small space allowed for water drainage (10 ft). About 7% of the total recharge flows through the saltstone block. Assuming this 7% is saturated with salt (Table 2) and is diluted by the other 93% of the water the N content of the water downflow of this landfill would be 4.0×10^3 ppm. This is much higher than the drinking water standard of 3.2 ppm* nitrogen for the nitrate/nitrite in decontaminated salt.

From the first model it was clear that a better disposal system would result if the large continuous clay cap was broken into smaller caps with spaces between for drainage. This would cause less perching of water resulting in less flow through the saltstone. Based on this observation variations on the original design were modeled (Table 1, Case B). In Case B-1 the saltstone blocks were in the same position and geometry but each block was capped individually with 10^{-9} cm/sec clay (Table 1). This eliminated the perching of water and reduced the flow of water through the saltstone to 2.1% of the total recharge (a N content of 1.1×10^3 ppm). In Case B-2 the same configuration was used again but the clay cap was assumed to be impermeable (Table 1). This did not change the fraction of recharge flowing through the saltstone since most of the flow was through the unprotected sides of the saltstone (Figure 5).

Landfill Designs With Individual Saltstone Blocks (Cases C-F)

The results of the first 3 calculations showed that individual blocks of saltstone, with space between for drainage, would perch

---

* The 3.2 ppm nitrogen drinking water standard is a weighted average for the nitrate/nitrite ratio in decontaminated SRP salt solution. The drinking water standard is 10 ppm for nitrate nitrogen and 1 ppm for nitrite nitrogen.

less water giving reduced water flow through saltstone and less leaching. These calculations also showed that a substantial portion of the recharge water flowing through the saltstone comes in through the unprotected sides of the blocks. The second series of landfills modeled included improved designs to protect the sides of the saltstone. Also an updated saltstone permeability number of 10^{-7} cm/sec was used (Table 3).

Case C was the same geometry as Case B but with the improved saltstone permeability of 10^{-7} cm/sec (Figure 1, Table 3). For this case the fraction of recharge flowing through the saltstone block was reduced to 7.3×10^{-4} yielding a N content of 39 ppm in the groundwater at the landfill boundary.

In Case D a trapezoidal saltstone block was used (Figure 1). With this design, water draining between blocks would be pulled toward the saltstone block only by soil suction* while gravity would tend to pull the water away from the saltstone surface. This design decreased the fraction of recharge water flowing through the saltstone to 2.3×10^{-4} for a N content in the groundwater of 12 ppm.

An extension of the clay cap to increase this umbrella effect to further protect the saltstone sides was used in Case E. This changed the flux through the saltstone block only slightly to 1.9×10^{-4}, 10 ppm N in the groundwater.

In Case F, the final case studied in this series, the saltstone was totally surrounded by 5 ft of 10^{-9} cm/sec clay (Table 3, Figure 10). This reduced the flow of water through the saltstone block substantially to 7×10^{-5} or 3.5 ppm N in the groundwater. This system reduces projected N releases from saltstone to near the drinking water standard of 3.2 ppm.

Landfill Designs With Improved Saltstone (Cases G, H, And I)

In the second series of calculations it was found that having an umbrella-like extension of the clay cap would decrease salt releases from saltstone. We also found that surrounding each block of saltstone with clay, although very expensive, would decrease salt releases to near drinking water standards.

The next series of calculations were done with landfill designs containing a newly developed and tested saltstone with a permeability of less than 5×10^{-10} cm/sec. Since the permeability of this new saltstone was lower than can be achieved

---

* In unsaturated flow capillarity tends to pull moisture from wetter into dryer areas and thus equalize moisture content.

with clay materials in the field, the idea of surrounding the entire block of saltstone with protective clay was abandoned. The protective barriers used in this final set of models were caps only, with different slopes and permeabilities. The trapezoidal geometry was used because of its benefit to inhibit leaching and because of construction limitations.

The first configuration modeled with the new saltstone was simply an unprotected trapezoidal block of saltstone (Case G, Table 4 and Figure 1). This design was modeled using 10^{-7} cm/sec and 5 x 10^{-10} cm/sec saltstone to check the feasibility of burying unprotected saltstone and as a base case to compare to designs with protective barriers. The trapezoidal block with a permeability of 10^{-7} cm/sec has 8.7 x 10^{-3} of the recharge water flowing through it yielding 466 ppm N in the groundwater. The block with a permeability of 5 x 10^{-10} cm/sec allows only 9 x 10^{-6} of the recharge water to flow through it, giving 0.5 ppm N in the groundwater. As expected 5 x 10^{-10} cm/sec saltstone would release much less contaminant than the 10^{-7} cm/sec saltstone surrounded by 10^{-9} cm/sec clay (Case F, Table 4).

In Case H the trapezoidal saltstone block was covered with protective clay caps of varying slope and permeability. The slope was added to the clay cap because it will help shed water and does not significantly complicate construction. The clay caps were 2 ft thick and extended 2.5 ft over the edge of the saltstone block.

These models showed again that the new low permeability saltstone (Case H-1, Table 3) allows much less salt release than the old formulation (Case H-2, Table 4). In this configuration 4.3 x 10^{-5} of the total recharge passes through the old formulation (2.3 ppm N), while only 4.5 x 10^{-7} of the recharge passes through the new low permeability saltstone (0.02 ppm N).

For designs with the low permeability saltstone covered with a clay cap, a 10^{-8} cm/sec clay cap is almost as effective as an impermeable (0 cm/sec) clay cap. A saltstone block covered with a 10^{-8} cm/sec clay cap with a 15% slope (Case H-2, Table 4) conducts 4.5 x 10^{-7} of the total recharge (0.02 ppm N). Decreasing the clay cap to 0 cm/sec permeability (Case H-3, Table 4) decreases the total recharge flowing through the saltstone to 3.4 x 10^{-7} (0.02 ppm N). This allows use of a 10^{-8} cm/sec cap if a lower permeability cap cannot be achieved easily and inexpensively.

The final design modeled by Intera was a block of saltstone protected by a gravel layer (Case I, Table 4). A gravel layer in an unsaturated zone diverts water by forming a capillary barrier through which water will not flow. This situation will persist

unless the zone above the gravel approaches saturation. The zone did not approach saturation with the geometry recharge rate and material properties used for this calculation, therefore, the gravel barrier was very effective. With a gravel barrier only 3.4×10^{-7} of the recharge water (0.02 ppm) flows through the saltstone. This is slightly less than the fraction which would flow through the saltstone with a 10^{-8} cm/sec clay cap (4.5×10^{-7}).

CONCLUSIONS

From the landfill designs modeled in this study it is clear that 1) protective caps reduce salt releases from saltstone, 2) clay caps covering individual saltstone blocks with plenty of drainage in between are more effective at reducing salt releases than are large caps covering several blocks, 3) extension of caps over the edge of saltstone blocks helps divert water away from the sides of the block, 4) saltstone with a permeability of 5×10^{-10} cm/sec or less, reduces nitrogen releases to well below drinking water standards.

Based on this study and consideration of costs and construction, 5×10^{-10} saltstone in a trapezoidal geometry with a 10^{-8} clay cap (Case H-2, Table 4) was chosen as the new reference saltstone landfill. In this design the saltstone block is 40.5 ft wide with the clay cap extending 2.5 ft over the edge. The space between clay covered blocks is 39 ft. Intera estimates that to allow adequate drainage without perching water the drainage space should be nearly as wide as the clay cap. With this design, all of the saltstone can be placed within the 100 acres available in Z-Area and all applicable standards of groundwater quality can be met. Expected chemical and radionuclide releases to the groundwater have been calculated based on the Intera modeling and SRL leaching studies and has been documented in another report.[3]

Experimental Program

To complement the computer modeling work, laboratory and field leaching experiments are being performed. Laboratory experiments include leaching of saltstone wasteforms in saturated (dip tests) and unsaturated (soil columns) situations to develop an understanding of contaminant release mechanisms from the saltstone. Field leaching experiments will provide data on salt release from several landfill systems. A one-tenth linear scale version of Case A (Figure 1) was placed in a lysimeter and data collection began in late 1982. Three additional landfill lysimeters will be completed in early 1983 with models of Cases G, H, and I (Figure 1).

The computer modeling, coupled with laboratory and field leaching experiments will provide a good overall picture of landfill leaching. Understanding landfill leaching will allow us to accurately predict salt releases from landfills.

QUALITY ASSURANCE

To assure that Intera personnel knew the exact details of the landfill designs to be modeled (geometries, protective barriers, material properties, etc.) meetings between Intera and interested SRL personnel were held before each round of calculations. The materials properties supplied to Intera by SRL were from documented studies.

The computer code used by Intera for this modeling work was compared to similar codes developed by other modelers. In addition, Intera has an internal crosscheck team which reviews and verifies all derivations, and calculations before documentation.

REFERENCES

1. "Parametric Modeling for Design of a Waste Disposal Facility," Report from Intera Environmental Consultants to E. I. du Pont. December 31, 1982. (Attached)

2. "National Interim Primary Drinking Water Regulations." U. S. Environmental Protection Agency. EPA 570/9-76-003.

3. M. D. Dukes. "Contaminant Release from Saltcrete," DPST-83-361. March 9, 1983.

MDD:ske
Disc 2

TABLE 1

ORIGINAL LANDFILL DESIGN

Case (See Fig 1)	Permeabilities (cm/sec)					Fraction of Recharge Through Saltstone	Concentration of N in Groundwater (ppm)
	Saltstone	Clay Cap	Clay Liner	Backfill	Host Soil		
A	10^{-6}	10^{-7}	10^{-6}	10^{-4}	10^{-3}	7×10^{-2}	4000
B-1	10^{-6}	10^{-7}	----	10^{-4}	10^{-3}	2.1×10^{-2}	1100
B-2	10^{-6}	0	----	10^{-4}	10^{-3}	2.1×10^{-2}	1100

1.0 INTRODUCTION

1.1 BACKGROUND

The disposal of chemical wastes to an engineered environment within the unsaturated zone is a commonly used landfill practice. For the Savannah River Plant (SRP) operated by E. I. du Pont de Nemours and Company for the U. S. Department of Energy, it is proposed that selected wastes be placed in designed landfill trenches on the plant site. The environmental performance of such a facility is very much a function of the waste, the site and the developed design.

The wastes at SRP are associated with special nuclear materials that are produced for national defense by irradiation in one of three production reactors at SRP. The irradiated material is separated into product and waste streams in one of two chemical separation plants. This process waste is stored in double-walled steel tanks, and has been accumulating for the 25 years the plant has been operating. Dupont plans to remove this waste from the tanks and incorporate the highly radioactive portion into a borosilicate glass, that will ultimately be shipped to a Federal repository. The bulk of the waste from the tanks, which consists principally of $NaNO_3$ and $NaNO_2$ salts, and NaOH, will be decontaminated to low levels of radioactivity. The reference process for disposal of this material consists of incorporating it into a specially formulated cement mix to form a saltcrete. This saltcrete will be poured into designed landfill trenches on the plant site. The saltcrete will have a low permeability to discourage leaching of the salts.

The principal environmental factor to be satisfied is that the concentration of dissolved salts in the ground water underlying the landfill facility should not exceed drinking water standards. As illustrated in Table 1, the primary constituent in the wasteform will be sodium nitrate, $NaNO_3$. The last column in the table indicates the chemical composition of the saltcrete leachate obtained in a laboratory test.

Table 1. Chemical Composition of Saltcrete and Leachate

(Provided by E. I. Dupont de Nemours and Company, 1982)

Compound	Bulk Waste Dry basis, wt %	Composition of Saltcrete, wt %	Composition of Leachate, wt %
$NaNO_3$	40	6	24.4
NaOH	19	3	3.9
$NaNO_2$	14	2	6.6
$NaAlO_2$	9	1.5	
Na_2CO_3	9	1.5	2.7
Na_2SO_4	8	1.2	8.0
$Na_2C_2O_4$	0.1	.015	
NaCl	0.2	.030	
Hg 0.05	.0076		
Miscellaneous	0.65	-	

The federal drinking water standard for nitrate (NO_3^-) is 44 mg/ℓ (10 mg/ℓ expressed as N). As can be noted from Table 1, the laboratory-obtained leachate has 24.4% by weight of $NaNO_3$, or roughly 286,700 mg/ℓ $NaNO_3$(assuming the leachage density is that of a 25% $NaNO_3$ water solution of 1.176 g/mℓ). Thus, the concentration equivalent to the drinking water standard for NO_3^- represents roughly a 4750 dilution ratio of the potential leachate. 286,700 mg/ℓ $NaNO_3$ is about 209,100 mg/ℓ of NO_3^-.

To meet drinking water standards in the underlying groundwater, a series of barriers to leachate migration have been considered. These include locating the saltcrete trenches in the zone of aeration above the water table, the low permeability of the saltcrete itself, along with low permeability liners surrounding the saltcrete monoliths, and the so-called "wick-effect". Before undertaking construction of such a facility, Dupont requested INTERA Environmental Consultants to undertake a quantitative study to evaluate various designs and design parameters, in order to insure that drinking water standards will be met. The study described in this report uses a computer simulation code to provide such a quantification for a number of different designs.

1.2 SIMULATION MODEL APPROACH TO EVALUATE DESIGNS

A saturated-unsaturated finite-element computer code of groundwater flow and dissolved constituent transport was used to evaluate the various designs. The designs were viewed in cross-sections taken perpendicular to the trenches, using symmetry when possible to reduce the computational burden, as shown in Figure 1. Each design was evaluated for steady-state flow. In some cases steady state and even transient simulations of constituent transport were also performed. Sensitivity analyses encompassing soil properties ranging from sand-like to clay-like were also performed. The computer code employed for these simulations is described more fully in Section 3.0.

1.3 DESIGN VARIATIONS TO BE EXAMINED

Dupont's original request for proposal and INTERA's response outlined a total of 30 separate cases to be simulated. The first 19 cases were design variations of a continuous clay cap over a grid of saltcrete monoliths with and without liners (eight monoliths per grid represneting eight trenches filled with saltcrete, as shown in Figure 1(a)). The next 4 cases were design variations of a discontinuous cap lying only over the saltcrete monolith as shown in Figure 1(b). The remaining 7 cases were to be selected later. In all cases examined, the saltcrete monoliths were installed in the zone of aeration above the water table.

After a reference case was completed and sensitivity runs were made over the range of uncertainty in soil properties, the continuous cap design were discarded as unsatisfactory. The continuous cap designs appeared to give no prospect of meeting the drinking water criteria. Subsequent analyses examined only the discontinuous cap variations. In articular, four different designs for individual monoliths in Figure 1(c) - 1(f) were evaluated.

Later laboratory studies at S.R.L. lead to the development of a modified saltcrete mixture with significantly lower permeability. A series of new designs for individual monoliths, shown in Figure 1(g) - 1(i), were evaluated incorporating this new material. A sloping cap and the use of gravel in the cap to create the so-called "wick-effect" were examined.

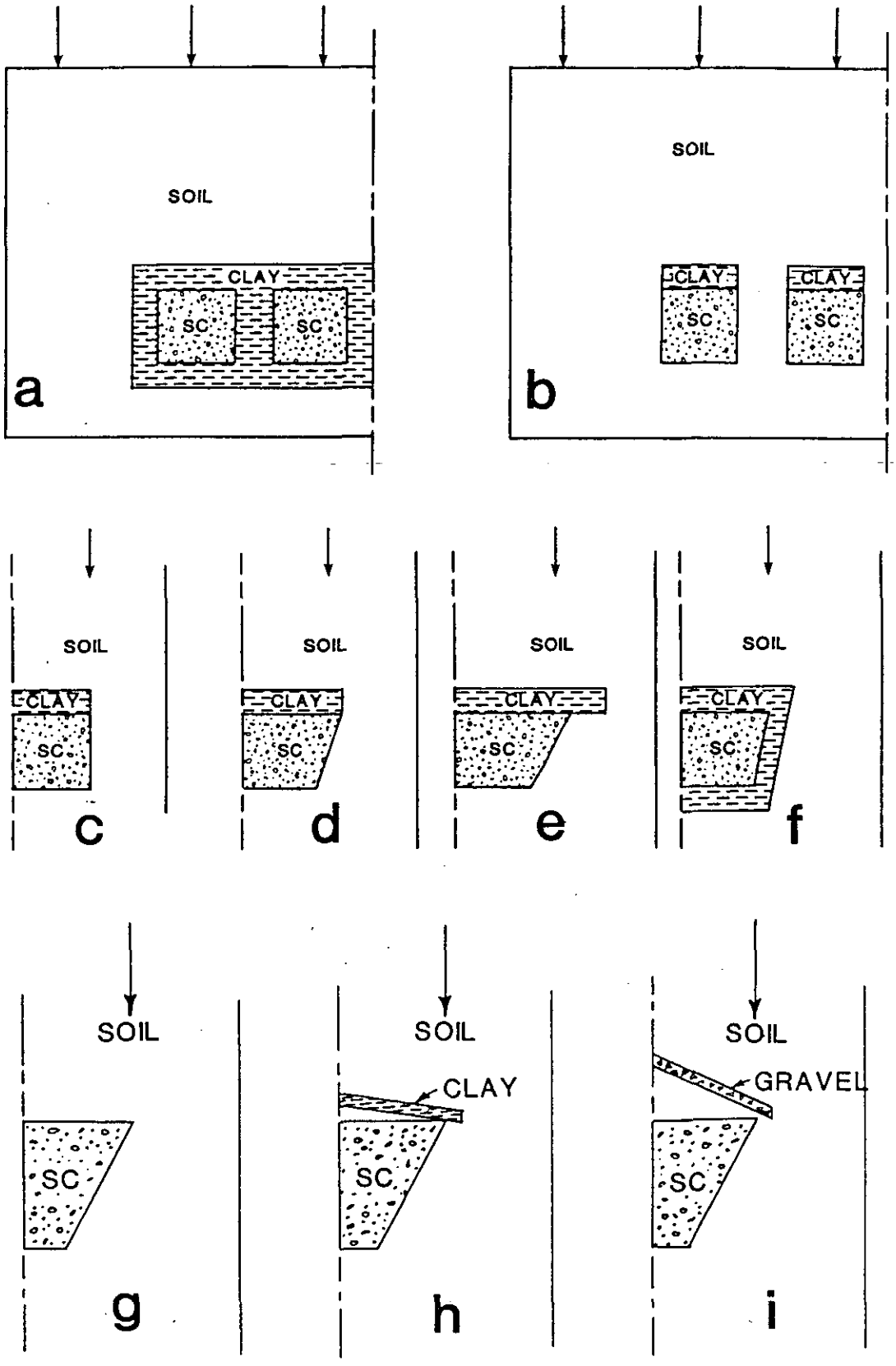

Figure 1 Modeled Geometries

1.4 DIVISION OF WORK BY TASKS

The evaluation work was divided into five primary tasks. These tasks included (1) data assimilation, (2) computer code modifications, (3) calculation of the reference case, and (4) calculations for the discontinuous cap cases, and (5) calculations for the new saltcrete material with clay and gravel caps. The data assimilation is described in Section 2.0. The modifications are detailed in Section 3.0. The calculations and evaluations are summarized in Section 4.0. Conclusions are given in Section 5.0. Recommendations are given in Section 6.0.

2.0 DESCRIPTION OF DATA BASE

Dupont has operated waste-producing facilities for some 25 years at the Savannah River Plant (SRP) site. During this time, a variety of soil-related data have been collected at the site. Generally, these soil measurements have been in the vicinity of existing waste facilities and thus are representative of the likely site chosen for the proposed saltcrete storage at SRL. To illustrate how these measured soil properties contrast to generic soil properties, the generic results are presented prior to the measured properties. The primary soil properties of interest are saturated hydraulic conductivity, unsaturated relative permeability and unsaturated capillary pressure.

2.1 GENERAL UNSATURATED SOIL PROPERTIES

Hillel (1977) has presented general soil property curves for a clay and sand soil types. These results are presented in Figure 2. These curves were obtained by assuming typical capillary pressure curves and calculating relative permeability (conductivity) relationships using characteristic functional forms. They are presented for comparison puposes only, and were never used in the simulations. Note that clay retains a higher percentage of water for high suctions than does sand. Similarily, even at low saturation sand's relative permeability can still be very large, compared to clay.

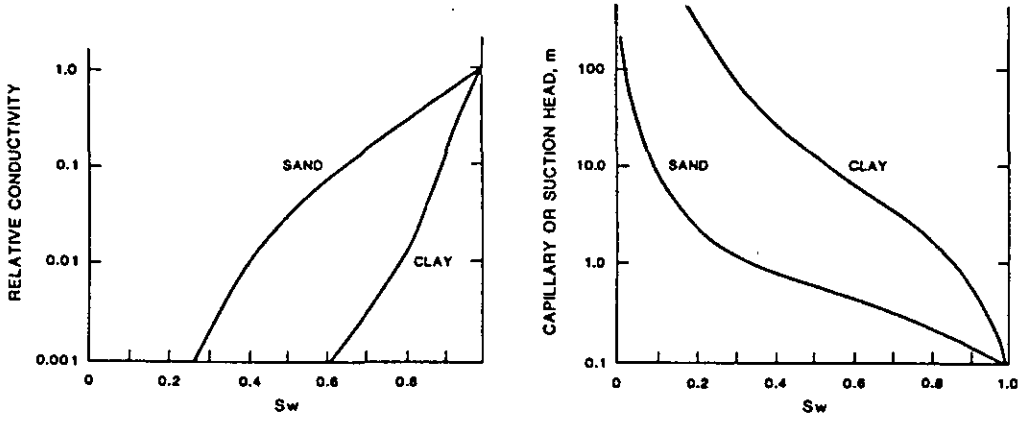

Figure 2. Generic Unsaturated Soil Properties for a Typical Clay and a Typical Sand.
S_w = saturation of water.

2.2 MEASURED SOIL UNSATURATED PROPERTIES

The measured SRP soil properties come from two primary sources. The first source was a Master's Thesis (Gruber, 1981) which described laboratory tests on soil cores, as well as field measurements. In Gruber's experiments, lysimeter tests were performed in soils at one of the waste sites and soil cores were analyzed in the laboratory. In these tests, relative permeability data were obtained at various soil depths below ground surface. We could find no clear-cut correlation of the relative permeabilities with depth (depths to 10 feet were obtained), and so have lumped all the available data. These results are illustrated in Figure 3(a). Data of capillary or suction pressure versus water content were also obtained. Once again, there was little difference in the depth (the top 10 feet), so the data were taken as independent of depth, and are presented later in Figure 4.

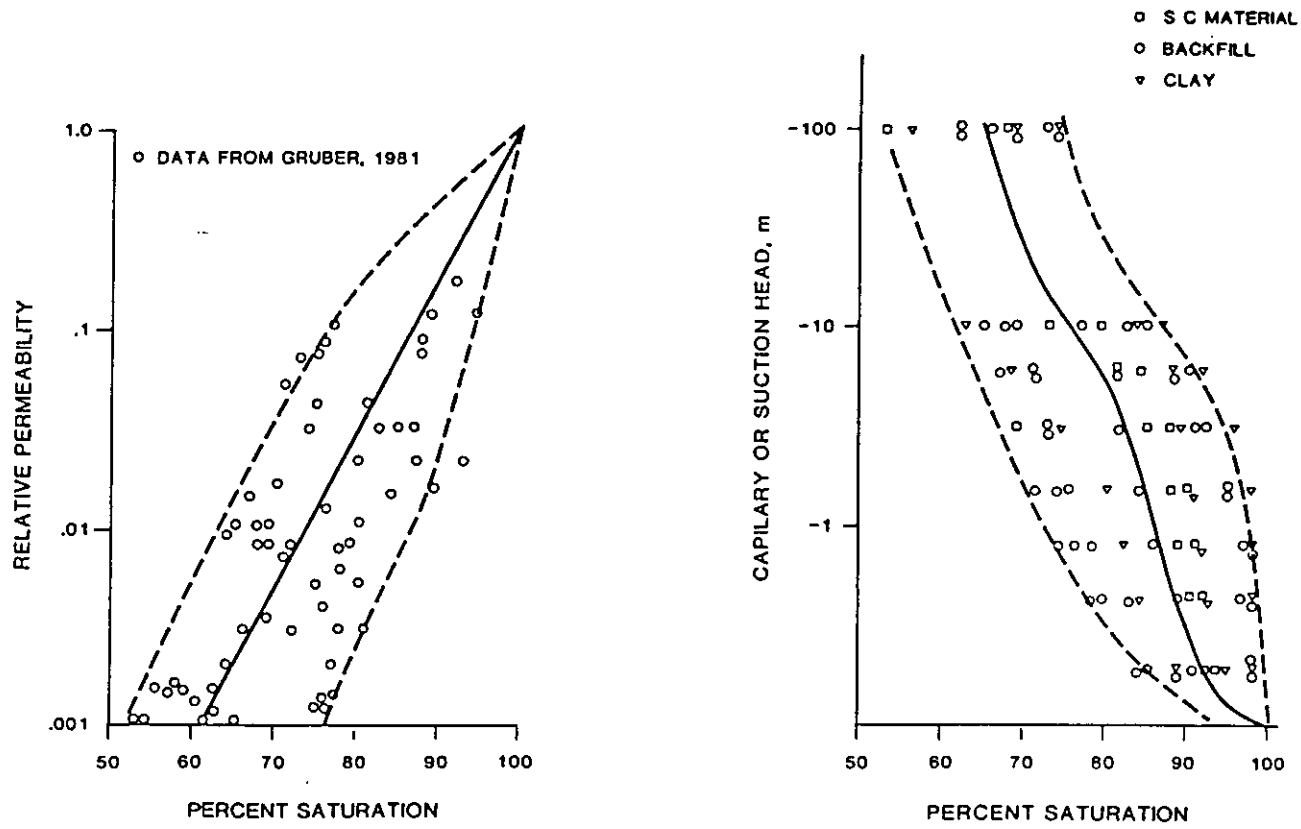

Figure 3. Unsaturated Soil Properties for Soils Near the Proposed Facility. The Solid Lines Represent the Properties used in the Simulation Runs. The Dashed Lines were used for Sensitivity Analyses

Additional capillary pressure or suction head data were gathered near the proposed saltcrete landfill facility by Root (1980). He sent a number of undisturbed soil samples from two holes, as well as compacted backfill material, for analysis. These data are shown in Figure 3(b). The samples could be classified as varying between silty sand and clay. Two samples have been omitted from Figure 3(b). One was classified as a silty sand, the other as a clay. Both samples looked much more like the depth averaged curve obtained by Gruber (1981). A comparison of these values is shown in Figure 4, along with the 12 sample data envelope for the remainder of Root's data. It should be noted that Gruber's soil samples were taken in the top 10 feet below the ground surface. The samples analyzed by Root were obtained in wells, and represented depths between 40 and 200 feet. These latter samples are probably more representative of soils which will control the water flow for the proposed saltcrete waste area.

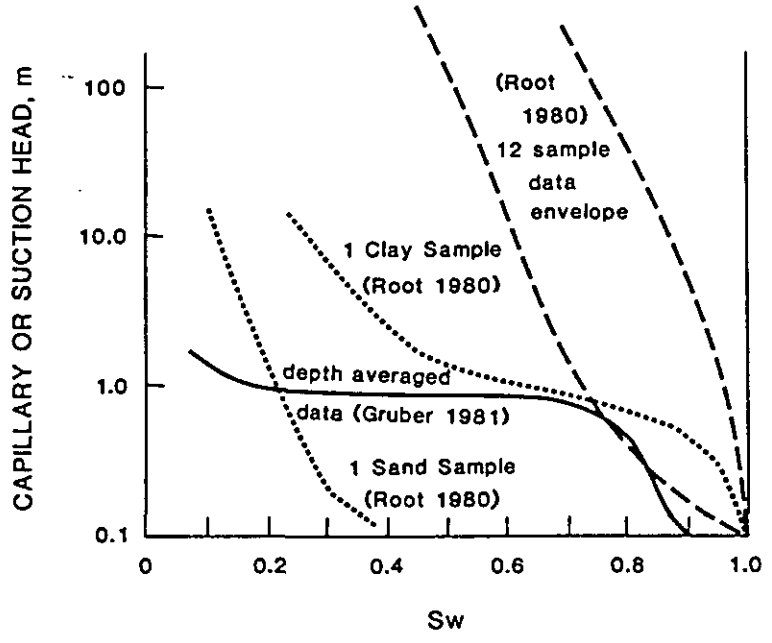

Figure 4. Comparison of Root's (1980) Unsaturated Capillary Pressure Data with Gruber's (1981) Data.

No capillary pressure data were available for the bentonite clay proposed for the cap and liner. However, since the measured soil curves were so strongly influenced by clay content, the properties represented by the 12-sample envelope of soils should adequately represent it.

If we accept the data presented by Root (1980), then the same unsaturated capillary pressure curve represented in Figure 3(b) can be used to represent (1) the host undisturbed soil, (2) the backfill soil, and (3) the clay cap/liner. Similarily the same relative permeability curve shown in Figure 3(a) can be used for all three materials. The solid lines represent the curves used. The dashed lines enveloping the data were used for sensitivity analyses.

2.3 UNSATURATED PROPERTIES FOR THE WASTE FORM

Several laboratories performing core measurements were contacted regarding capillary pressure and relative permeability data for the saltcrete waste form. Even data for concrete capillary pressure was unavailable. We then looked for data for analogous materials.

As an example, a low permeability limestone capillary pressure curve (3 millidarcy or $3x10^{-6}$ cm/sec) is shown on a plot in Figure 5 and compared to the Root data envelope. It illustrates that for capillary or suction pressures up to 10-20 meters, the limestone curve is very similar to the upper envelope of the Root data. At higher suctions the limestone saturation drops off significantly.

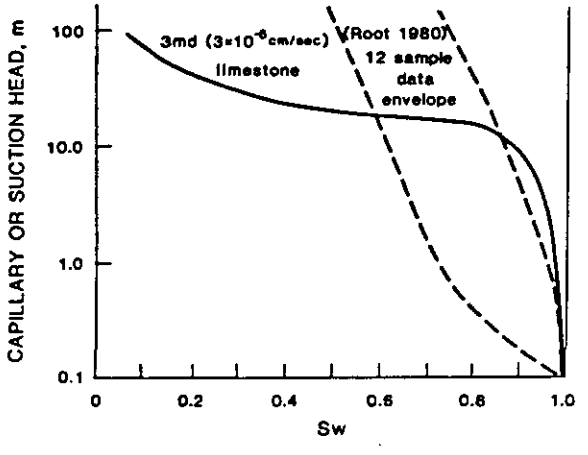

Figure 5. Comparison of Limestone and Root's Soil Capillary Pressure Curves.

We assumed that the limestone and saltcrete behaviors are similar since the saltcrete will probably be within 20 m of the water table, the capillary pressure curves controlling the saltcrete behavior should look very much like the soil properties. As a consequence, we have chosen to represent the waste form by the properties within the soil property envelope.

2.4 SATURATED HYDRAULIC CONDUCTIVITY

The saturated hydraulic conductivity values for the various soils and materials was specified by duPont. The values used are given in Table 2. The host soil value represents typical soils at the site (a lower value was used for the simulations in Section 4.2.2). The lower backfill conductivity represents the effects of a carefully compacted backfill. The clay cap and liner values reflect evolving estimates for the type of material and compaction possible for the site and various designs. The gravel gap estimate is estimated for a fine "pea" gravel. The saltcrete values are based on laboratory experiments. The final value of 5×10^{-10} cm/sec reflects the recent development of a special mixture for low conductivity saltcrete. These properties are assumed to be isotropic.

Table 2. Saturated Hydraulic Conductivity Values, cm/sec

Material	Reference Case (4.1)	Discontinuous Cap (4.2.1)	Single Monolith (4.2.2)	Single Monolith (4.3)
Saltcrete	10^{-6}	10^{-6}	10^{-7}	5×10^{-10}
Clay Cap	10^{-7}	10^{-9}	10^{-9}	10^{-8}
Clay Liner	10^{-6}	10^{-6}	10^{-6}	NA
Gravel Cap	NA*	NA	NA	10^{+1}
Backfill	10^{-4}	10^{-4}	10^{-4}	10^{-4}
Host Soil	10^{-3}	10^{-3}	10^{-4}	10^{-3}

*NA = not applicable

3.0 DESCRIPTION OF MODEL USED

The analyses involves water flow in the partially saturated zone of aeration above the water table and the leaching of the salt(s) from the saltcrete waste form to be transported down to the water table. A quantitative assessment of water flow could include modeling of the two phase flow system of air and water in the zone of aeration. However, water flow in the near ground surface region is usually adequately described by a simplification of full two phase flow. This simplification assumes that the air phase remains at gravity equilibrium (i.e., the gas phase pressure is equal to atmospheric pressure at the surface and increases by the air density below the surface). The development can easily be illustrated in the following equations.

$$- \nabla \cdot \rho_g v_g = \frac{\partial(\phi \rho_g S_g)}{\partial t} \tag{1}$$

$$- \nabla \cdot \rho_w v_w = \frac{\partial(\phi \rho_w S_w)}{\partial t} \tag{2}$$

where: ρ_g, ρ_w = densities of gas and water phases

S_g, S_w = saturation of gas and water phases

v_g, v_w = Darcy velocity of gas and water phases

and ϕ = porosity

$$v_g = - \frac{k\, k_{rg}}{\mu_g} (\nabla p_g - g \rho_g \nabla d) \tag{3}$$

$$v_w = - \frac{k\, k_{rw}}{\mu_w} (\nabla p_w - g \rho_w \nabla d) \tag{4}$$

where: k = saturated instrinsic permeability

k_{rg}, k_{rw} = relative permeability of gas and water

p_g, p_w = phase pressures of gas and water

d = depth

and g = gravitational constant

Equation (2) could have been written in terms of water content $\theta = \phi S_w$ where ϕ is porosity.

The two flow equations are coupled by the definition of capillary pressure and saturation:

$$p_c = p_g - p_w = f(S_w) \tag{5}$$

$$S_w + S_g = 1.0 \tag{6}$$

If the gas pressure is hydrostatic, $p_g \equiv \rho_g d$, then from Equation (1) we have

$$v_g = 0$$

and from Equation (4) we have:

$$v_w = \frac{k\, k_{rw}}{\mu_w}(\nabla p_c - g\Delta\rho\nabla d)$$

where $\Delta\rho = \rho_w - \rho_g \cong \rho_w$. Then assuming the water density is essentially constant, Equation (2) can be written approximately as:

$$\nabla \cdot \frac{k\, k_{rw}}{\mu_w}(\nabla p_c - g\rho_w \nabla d) = \frac{1}{\frac{dp_c}{d\theta}} \frac{\partial p_c}{\partial t} = \left(\frac{d\theta}{dp_c}\right)\frac{\partial p_c}{\partial t} \tag{7}$$

where $\theta \equiv \phi S_w$ is the water content. The term $d\theta/dp_c$ is referred to as specific moisture capacity.

Equation (7) is called the "Richards" equation or single phase approach to partially saturated flow problems. It models both saturated and unsaturated soils. The actual saturated-unsaturated computer code used is described in the following paragraphs.

3.1 THE SATURATED-UNSATURATED COMPUTER CODE USED

To model flow and mass transport in two-dimensional variably saturated cross-sections, INTERA used modifications of the (Reeves and Duguid, 1975; Duquid and Reeves, 1976) Galerkin finite element code as well as the follow on FEMWATER-FEMWASTE codes (Yeh and Ward, 1980). The model(s) can use both three node triangular elements and four node isoparametric quadrilateral elements.

Integration of the Galerkin equations is performed using a Gauss-Legendre Quadrature. Solution of the assembled linearized matrix equations is by Gauss elimina- tion. The code is well documented and has been used by INTERA and many others for the analysis of field problems. At INTERA, the code is operational on the CDC CYBER 176 and the vector processor 205 machines.

The Duguid and Reeves (Reeves and Duguid, 1975; Duguid and Reeves, 1976) code solves the flow equation for two-dimensional cross-sections with input parameters including: the saturated hydraulic conductivity tensor; relative permeability as a function of the moisture content; specific moisture capacity derived from the pressure head-moisture content relationship; fluid density and compressibility coefficients; formation compressibility coefficient; and porosity. Initial conditions for transient analysis and a wide variety of boundary condition types are also inputs to flow analysis. Through the use of Darcy's Law, velocities can be determined from pressure distributions. The code can be readily used to describe both anisotropic and heterogeneous porous media.

One of the fundamental differences between the original Duguid-Reeves code and the subsequent FEMWATER codes is the manner in which water velocities are calculated. Yeh and Ward (1980) in developing FEMWATER decided that the model could be improved by using the Galerkin technique to directly calculate the velocities at the nodes, in contrast to the original code which calculated velocities at the Gauss points and interpolated for velocities at the nodes. This new approach was shown to improve the material balance calculations around elements for certain problems. We had difficulties with this technique where several orders of magnitude contrast in hydraulic conductivity exist between the elements, as in the case of the interface of saltcrete and soil. Consequently, the element velocity values were used for the results reported herein.

The mass transport equation in the variably saturated Duguid and Reeves (1976) code includes parameters for longitudinal and transverse dispersivities as well as coefficients that permit the description of attenuation and decay for nonconservative species. Leach models have been developed for the mass transport system. A variety of boundary conditions are possible in the transport model.

3.1.1 Modifications Added by INTERA

Both the Duguid-Reeves and FEMWATER codes use the same update of the nonlinearities in the Richards Equation (Eq. 7). There are nonlinearities on both the space derivative side, $k_{rw} = f_1(S_w) = f_2(p_c)$, and the time derivative side, $\frac{dp_c}{d\theta} = f(\theta)$. These non linearities are updated on the space side of the equation by resubstitution after each iteration.

For a steady state flow problem, only the space derivative side is important. For the special case of one-dimensional flow subject to a constant flux boundary condition at the surface, Equation 7, has the form:

$$K\, k_{rw} \left(\frac{\partial h_c}{\partial z} - 1\right) = Q \qquad (8)$$

where now K = the saturated hydraulic conductivity = $k\rho g/\mu$, ℓ/t,

k_{rw} = the dimensionless relative conductivity, a function of water saturation

h_c = the suction head, $\ell = p_c/\rho w g$

Q = flux rate at the surface, $\ell^3/\ell^2 t$

The difficulty of trying to solve Equation (8) by a resubstitution technique can easily be deduced by examining the resulting ordinary differential equation.

The iterative version of (8) is written as:

$$K k_{rw}^{\ell+1} \left(\frac{\partial h_c^{\ell+1}}{\partial z} - 1\right) = Q \qquad (9)$$

where ℓ = the iterate. Using explicit resubstitution to update the non-linearity, as in the standard versions of these computer codes, the value or relative permeability is taken from the final calculation of the previous iteration:

$$k_{rw}^{\ell+1} \simeq k_{rw}^{*\ell} = k_{rw}(S_w^{\ell}) = k_{rw}(h_c^{\ell}) \qquad (10)$$

in which $S_w^{\ell} = S_w(h_c^{\ell})$. The resulting solution at an arbitrary height, z is:

$$h_c^{\ell+1} = h_{c_o} + \int_o^z \left(\frac{Q}{Kk_{rw}^{*\ell}} + 1\right) dz \qquad (11)$$

in which $h_{c_o} = h_c$ at $z \cong 0$ (i.e., a held saturation at the lower boundary).

Suppose the bottom boundary is the water table, such that $S_w = 1.0$ and $h_c \cong 0$. The suction head profile h(z) can be deduced to look conceptually like that shown in Figure 6. The slope of $\frac{\partial h_c}{\partial z}$ must by Equation (9) approach $(\frac{Q}{K} + 1)$ in the vicinity of the water table ($k_{rw} = 1.0$). Further, high above the water table h_c becomes constant, and here k_{rw} must approach $\frac{Q}{K}$. If the portion of the above problem near the water table is neglected, it is relatively easy to show by numerical experiment that Equation (11) diverges for reasonable non-linearities in k_{rw} (S_w).

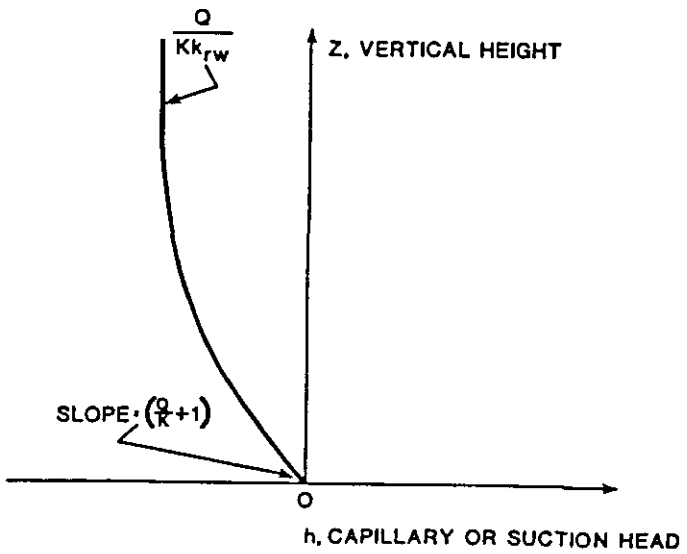

Figure 6. Suction Head Solution for a Constant Infiltration Rate.

The change made in both the Duguid-Reeves and FEMWATER codes has been to introduce an update method for the nonlinearilty on the space derivative side of Equation (7). This update introduces a weighting factor to multiply the current k_{rw} and the previous k_{rw} to use for the next iteration. Essentially, the algorithms can be expressed in the following steps:

(1) For each iteration $\ell+1$ calculate the relative permeability using the latest estimate of suction head, h_c^{ℓ}: $k_{rw}^{*\ell} = k_{rw}(h_c^{\ell})$

(2) Compare this value to the relative permeabiity k_{rw}^{ℓ} used to find h_c^{ℓ}:

(a)	(b)	(c)	(d)
If $k_{rw}^{*\ell} > k_{rw}^{\ell}$	If $k_{rw}^{*\ell} > k_{rw}^{\ell}$	If $k_{rw}^{*\ell} < k_{rw}^{\ell}$	If $k_{rw}^{*\ell} < k_{rw}^{\ell}$
and $k_{rw}^{*\ell-1} < k_{rw}^{\ell-1}$	and $k_{rw}^{*\ell-1} > k_{rw}^{\ell-1}$	and $k_{rw}^{*\ell-1} > k_{rw}^{\ell-1}$	and $k_{rw}^{*\ell-1} < k_{rw}^{\ell-1}$
then $\beta^{\ell} = \alpha\beta^{\ell-1}$	then $\beta^{\ell} = \beta^{\ell-1}$	then $\beta^{\ell} = \alpha\beta^{\ell-1}$	then $\beta^{\ell} = \beta^{\ell-1}$

(3) $k_{rw}^{\ell+1} = (1 - \beta^{\ell})k_{rw}^{\ell} + \beta^{\ell} k_{rw}^{*\ell}$

(4) Update $h_c^{\ell+1}$ from Equation (7)

(5) repeat (1) through (4) until convergence.

The values of α and β^{o} are chosen between zero and one. Obviously β starts near unity and decreases toward zero as convergence is approached (providing the new k_{rw} begins to alternately overestimate and underestimate the true value). At convergence, the old iterate value k_{rw}^{ℓ} is used. The degree of convergence can easily be checked by calculating the norm $[k_{rw}(h_c^{\ell+1}) - k_{rw}(h_c^{\ell})]$ which should be near zero.

3.1.2 Graphics Added

The original request for proposal outlined some 30 parameteric cases. In order to be able to plot these and subsequent results for comparative purposes, a graphics package was added to the model. This graphics package

allowed plotting of (1) suction head; (2) total head; (3) water content; (4) concentrations; and (5) particle pathlines as two dimensional graphs. Results will be illustrated in the results section. The pathline program was limited to orthogonal finite element meshes and was not used for the trapezoidal meshes of Sections 4.2.2 and 4.3.

3.1.3 Verification Tests

Prior to conducting a parametric variation over a range of variables for a specific problem, it is a good practice to compare the model with a similar analytical verification test. Verification in the sense used here implies a check that the model is programmed to meet the required design specifications. The word validation would here imply that the model adequately represents the physical problem for which its performance specifications were developed. Although this section will address primarily the verification step conducted for this project, we strongly support a future validation comparison with an on site field experiment.

The simple verification test can be described as follows:

(1) at $z = 0$, $k_{rw}(S_w) = \frac{Q}{K}$

(2) at $z = L$, the infiltration, Q, was 40 cm/yr (1.27×10^{-6} cm/sec) and this water contained no contaminant

(3) at $x = 0$, $C = C_o$

(4) for large x, $C \to 0$

It involves uniform steady flow vertically downward in the z direction, and steady transverse dispersion of a dissolved salt in the horizontal direction. The saturation profile is uniform.

The analytical solution to this problem can be expressed as:

(1) $S_w = \text{constant} = S_w(k_{rw} = \frac{Q}{K})$

(2) $h_c = \text{constant} = h_c(S_w)$

$$(3)\quad C = C_o \operatorname{erfc}\left[\frac{x}{\left(\frac{4\theta Dz}{w}\right)^{1/2}}\right]$$

where w = the vertical Darcy velocity = Q, ℓ/t

and D_T = the transverse dispersion coefficient, $\alpha_T \frac{w}{\theta} + D_m$, ℓ^2/t

α_T = the transverse dispersivity, ℓ

D_m = molecular diffusion coefficient = $D_m(\theta)$, ℓ^2/t

The model was compared with this analytical solution for two quite different values of D_T. The results for the two D_T values were identical when scaled by depth. The results for one experiement are illustrated in Figure 7.

3.2 LIMITATIONS

The finite element model (or any discrete approximation) model is subject to limitations in the choice of element size and/or time step. The following guidelines were used to set the element size, where Δx and Δz are the characteristic dimensions of an element, and assuming that the predominant flow is vertically downward.

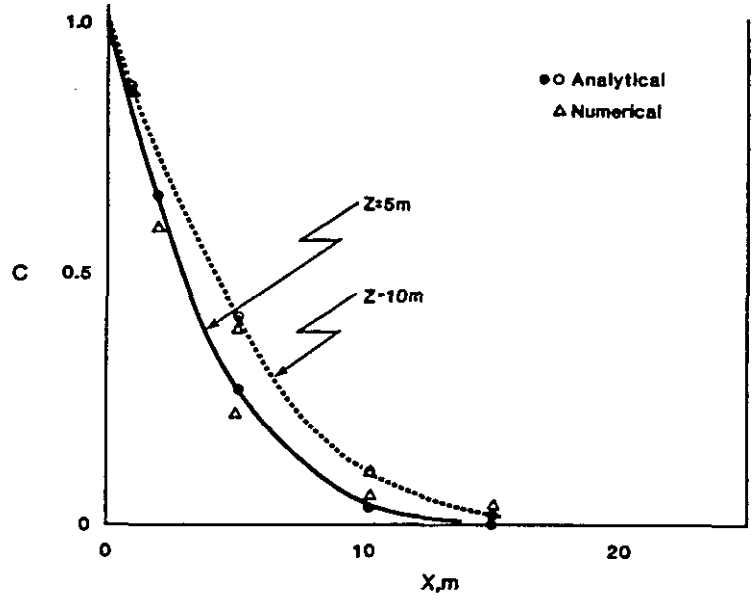

Figure 7. Comparison of Analytical and Numerical Results.

Water Flow Equation

1. To avoid overshoot and undershoot

$$\Delta z \leq 2\phi K_w / \left(\frac{dh_c}{dS_w} \frac{dk_{rw}}{dS_w}\right)$$

2. To get accurate capillary (saturation) gradient normal to flow

$$\Delta x \leq \phi K_w L_z \left(\frac{dh_c}{dS_w} \frac{dk_{rw}}{dS_w}\right)$$

Transport Equation (neglecting molecular diffusion)

1. To avoid overshoot and undershoot (α_L = longitudinal dispersivity).
   $\Delta x, \Delta z \leq 2\alpha_L$
2. To get accurate diffusion solution in direction transverse to flow
   $\Delta x \leq \alpha_T L_z$

3. For central in time approximations:
   (a) $\Delta t \leq \alpha_L \theta / w$
   (b) $\Delta t \leq (\Delta z^2 / \alpha_L w)$ (since the predomant velocity is vertical)

The above relations come from analyses of second order correct finite difference approximations. They need not be satisfied exactly. We have found finite element (first order basis function) approximations require almost the same element block and time step criterion.

All of the relations above depend upon either the capillary or suction head or the dispersivity. The dispersivity magnitude depends on the transport distance L_z. Here, the distance from the saltcrete to the water table varies over about 5 - 15 m. The curves summarized by Grisak and Pickens (1980) indicated a dispersivity of 1 - 2 meters is the appropriate range. Thus element lengths in the 2 - 4 m range are appropriate.

The capillary head curves presented earlier indicate that the equilibrium capillary transition zone would be on the order of at least 10 m vertically. As a consequence, element sizes of 2 - 4 m would again describe the transition zone adequately.

4.0 CALCULATED RESULTS

4.1 GENERAL EVALUATION OF A CONTINUOUS CLAY CAP - THE REFERENCE CASE

The design chosen by duPont for the reference case consisted of a grid of eight saltcrete monolithes (10 m x 10 m), a continuous clay cap (2 m thickness) under 12 meters of backfill, a clay side between adjacent waste grids (2 m thickness), a bottom liner (2 m), backfill between saltcrete monolithes (2 m width) and a depth to the water table of 2 m below the liner. The reference case finite element mesh of 28 x 22 elements and properties used are shown in Figure 8 (see also Figure 1a). The reference case includes a prescribed infiltration rate of 40 cm/yr on the top boundary;

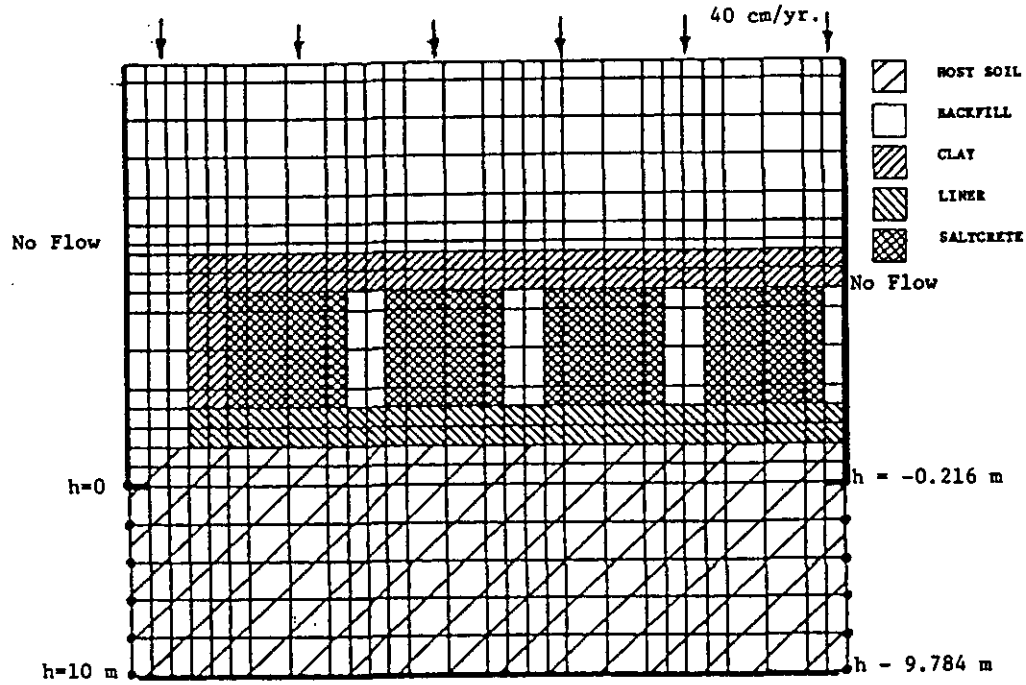

Figure 8. Reference Case Grid.

no flux bundaries of symmetry on the right and left, within the zone of aeration; prescribed head boundaries in the zone of saturation inducing a net saturated flow from left to right to simulate ambient site conditions; and a no flux boundary below. The properties of each media are given in Table 2. Assumed porosities were 40% for the backfill and host soilds, and 60% for the clay cap. These values were specified by duPont except for the porosity of saltcrete. This value was taken as 10%. The porosities specified for host rock and backfill were probably total porosity rather than effective porosity. The data of Root (1980) indicates that the effective porosity of soil and backfill to be more in the range of 20%. The steady-state flow calculations will be unaffected by this change. However, the transport times calculated should probably be considered high by about a factor of two. Steady state flow, steady and transient salt transport and a sensitivity analyses were run.

4.1.1 Steady State Simulation

The results presented are for both steady state flow and steady state transport calculations. Transient transport is presented in the next section and transient flow subsequently. The results presented include:

- o flow stream lines (pathlines)
- o water saturation results
- o pressure head (negative suction head)
- o steady state concentration profiles

Nine separate streamlines are shown in Figure 9. The starting positions of these streamlines was selected in order to divide the incoming infiltration flow into ten equal parts. Notice that less than two-tenths of the flow went through the waste form grid while more than eight-tenths went through the area between the adjacent grids. This could be expected from a simple consideration of the average hydraulic conductivities the water would encounter along various paths from the ground surface to the water table. The correct average conductivity at steady state can easily be shown to be the harmonic mean of the conductivity paths. The only difficulty with a simple analysis of this type is that the water saturation is unknown and so also is the relative permeability. Assuming saturated conditions at least allows us to compute a rough approximation of the net harmonic mean along various pathlines.

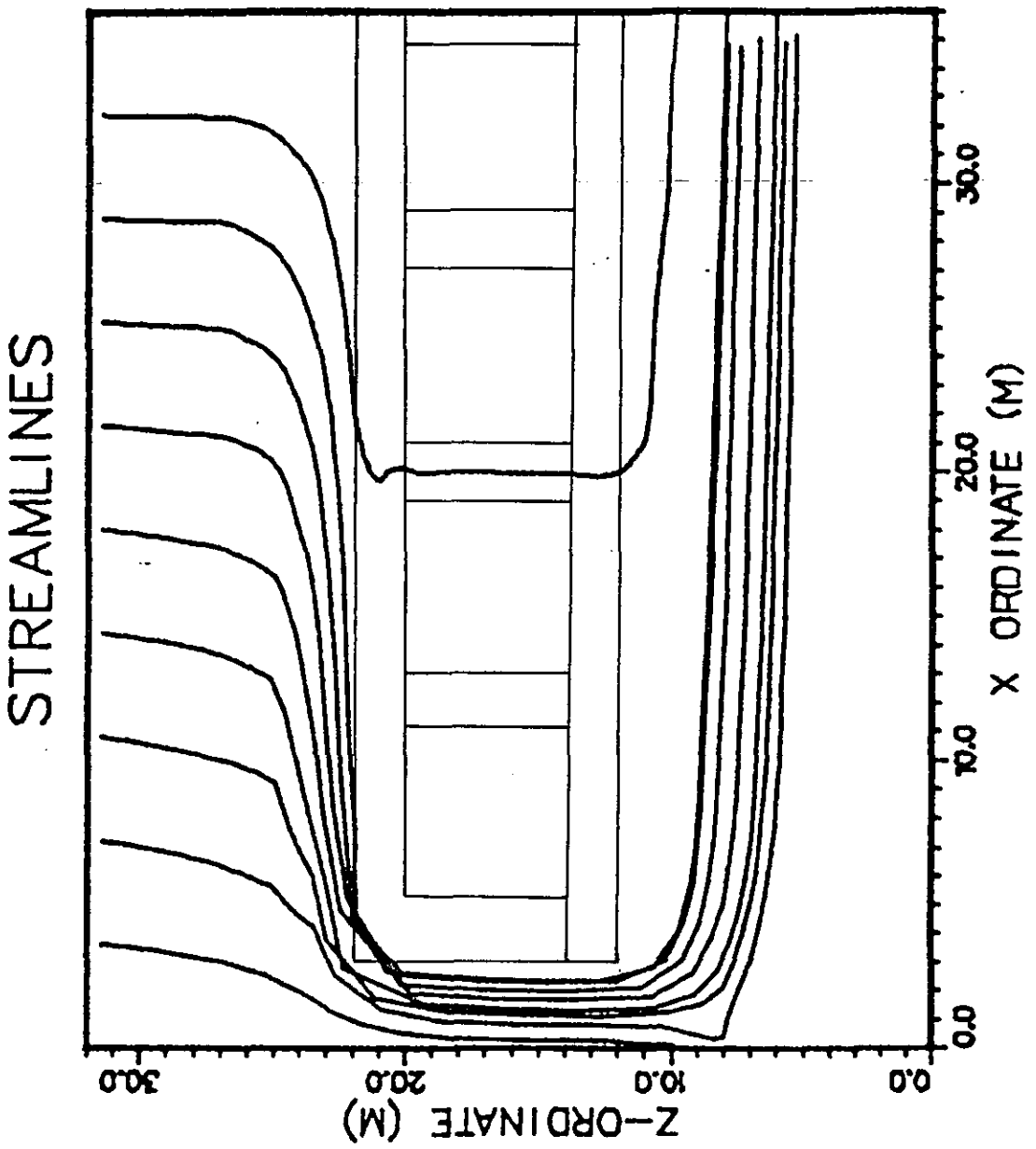

Figure 9. Reference Case Streamlines.

We consider here just three such path lines:

1. The pathline through the opening between grids.
   The average hydraulic conductivity should be:

$$\bar{K} = \frac{26 + 2}{\frac{26}{10^{-4}} + \frac{2}{10^{-3}}} = 1.07 \times 10^{-4} \text{ cm/sec}$$

   where 28 m is the depth to water table, composed of 26 m of backfill and 2 m of host soil.

2. The pathlines through the backfill between saltcrete waste blocks should have a net average conductivity of:

$$\bar{K}_2 = \frac{12 + 2 + 10 + 2 + 2}{\frac{12}{10^{-4}} + \frac{2}{10^{-7}} + \frac{10}{10^{-4}} + \frac{2}{10^{-6}} + \frac{2}{10^{-3}}} = 1.26 \times 10^{-6} \text{ cm/sec}$$

   where there are 12 m of overburden backfill, 2 m of cap, 10 m of backfill between blocks, 2 m of liner and 2 m of host soil.

3. The pathline through the saltcrete waste forms would have an approximate conductivity of:

$$\bar{K}_3 = \frac{12 + 2 + 10 + 2 + 2}{\frac{12}{10^{-4}} + \frac{2}{10^{-7}} + \frac{10}{10^{-6}} + \frac{2}{10^{-6}} + \frac{2}{10^{-3}}} = 8.7 \times 10^{-7} \text{ cm/sec}$$

   where there are 12 m of overburden backfill, 2 m of cap, 10 m of saltcrete, 2 m of liner, and 2 m of host soil.

The net flow through each of these paths should be approximately the product of the average hydraulic conductivity and the area through which the flow occurs. The ratio of the flow through the waste form can then be approximated as:

$$\frac{Q_{2,3}}{Q_{Total}} = \frac{(1.26 \times 10^{-6})\ 7 + (8.7 \times 10^{-7})\ (40)}{(1.07 \times 10^{-4})\ 3 + (1.26 \times 10^{-6})7 + 8.7 \times 10^{-7}\ (40)} = 0.12$$

The above simplified analyses, assuming uniform flow and saturated conditions, indicates that about 12% of the flow should go through the waste form grid rather than the roughly 20% shown in the figure. Of course the water saturation is not uniform across the cross-section. As will be seen later a region of high water content occurs above and in the clay cap which accounts for the higher flow through the waste form grid than calculated simply as above.

The actual flow through the saltcrete monoliths themselves in given by:

$$\frac{Q_3}{Q_{Total}} = \frac{(8.7 \times 10^{-7})\ (40)}{(1.07 \times 10^{-4})\ 3 + (1.26 \times 10^{-6})\ 7 + 8.7 \times 10^{-7}\ (40)} = 0.095$$

Thus, approximately 9.5% of the water flows through the saltcrete monoliths, themselves. This is later referred to as the saltcrete flux. The actual value of this volumetric flux calculated from numerical integration of the simulation results is 7.5%.

One of the streamlines shown in the Figure 8 actually exits at the upstream end. This is possible since a pressure head boundary condition was set at the upstream end of the saturated zone, and a great deal of the infiltration flow has been diverted to this side.

The next figure, Figure 10, illustrates a plot of pressure head (negative capillary or suction pressure). The area above the clay cap is at zero or positive pressure indicating it is water saturated. Below the water table the head is also positive with only a slight gradient in the positive x direction. The backfill between saltcrete monoliths is a bit drier than the open area around the waste grid.

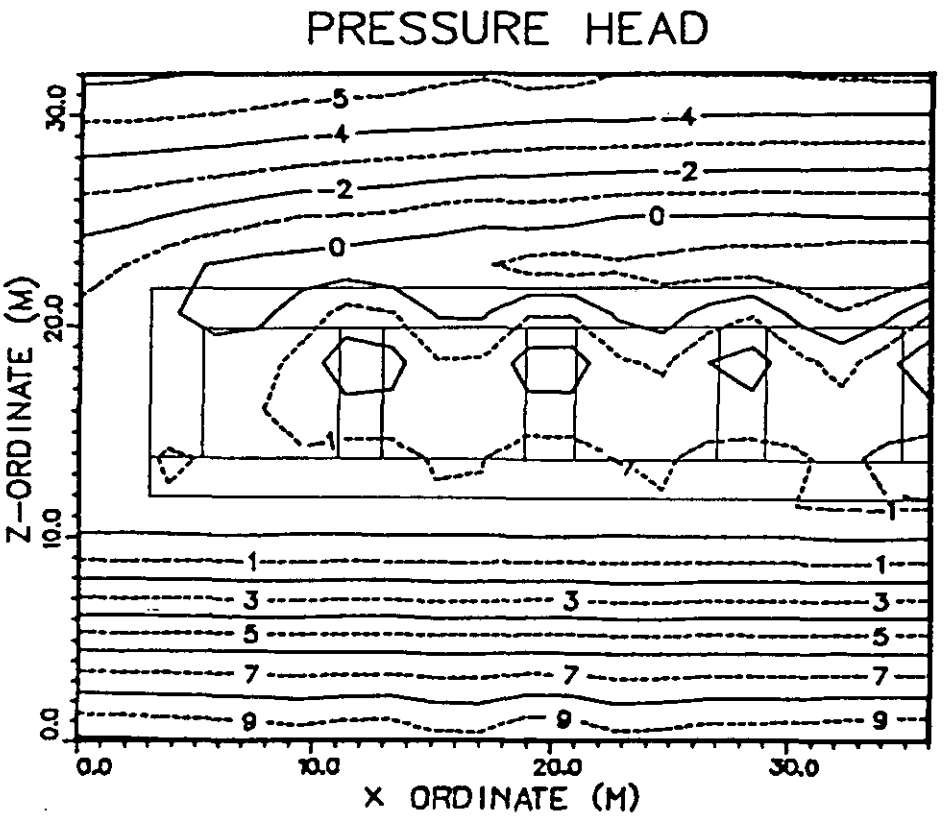

Figure 10. Pressure Head for the Reference Case.

The water saturation (rather than water content) is shown in Figure 11. In this plot the printer character 0 indicates water saturations of essentially 100%. Note that even at ground surface the water saturation is just over 80%. The saturated areas are above the clay cap and below the water table.

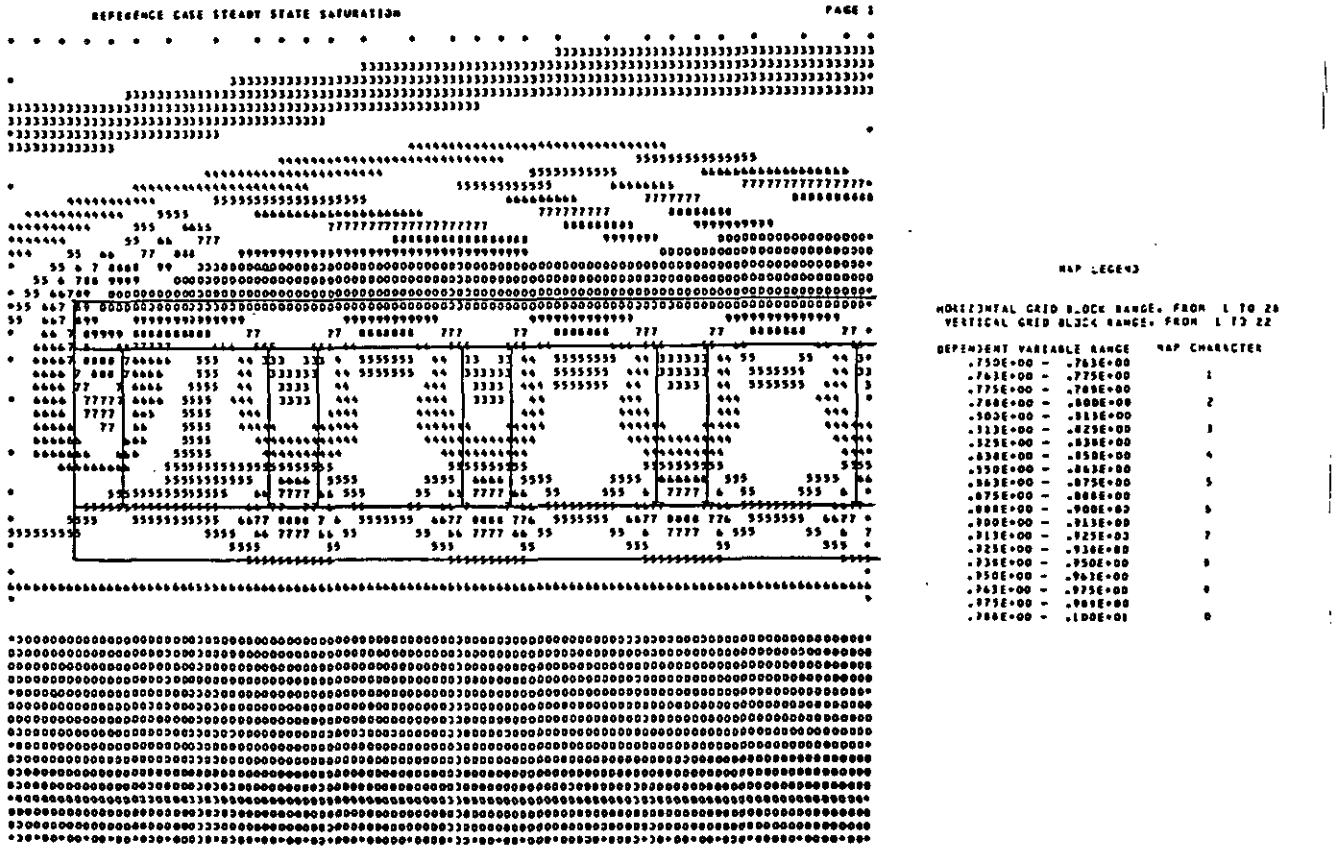

Figure 11. Water Saturation for the Reference Case.

The calculated steady state salt concentrations are illustrated in Figure 12. The boundary conditions used for these calculations were to hold the saltcrete monoliths at a dimensionless concentration of unity. In this case the flow through the saltcrete would exit with unit concentration obviously representing the nitrate saturated leachate, 209,100 mg/ℓ. It should be noted that the concentrations upstream from the waste saltcrete are somewhat artificial. The dispersivity value used, 2 m, although representative of the downstream flow distances here also causes increased diffusion upstream. The concentrations upstream then probably should be neglected. The concentrations in the water below the water table however significantly exceed the drinking water standard. Thus, unless the transient calculation indicates that the time to steady state takes much longer than the time to leach out the salt content of the saltcrete, it appears that the continuous clay cap design is not viable.

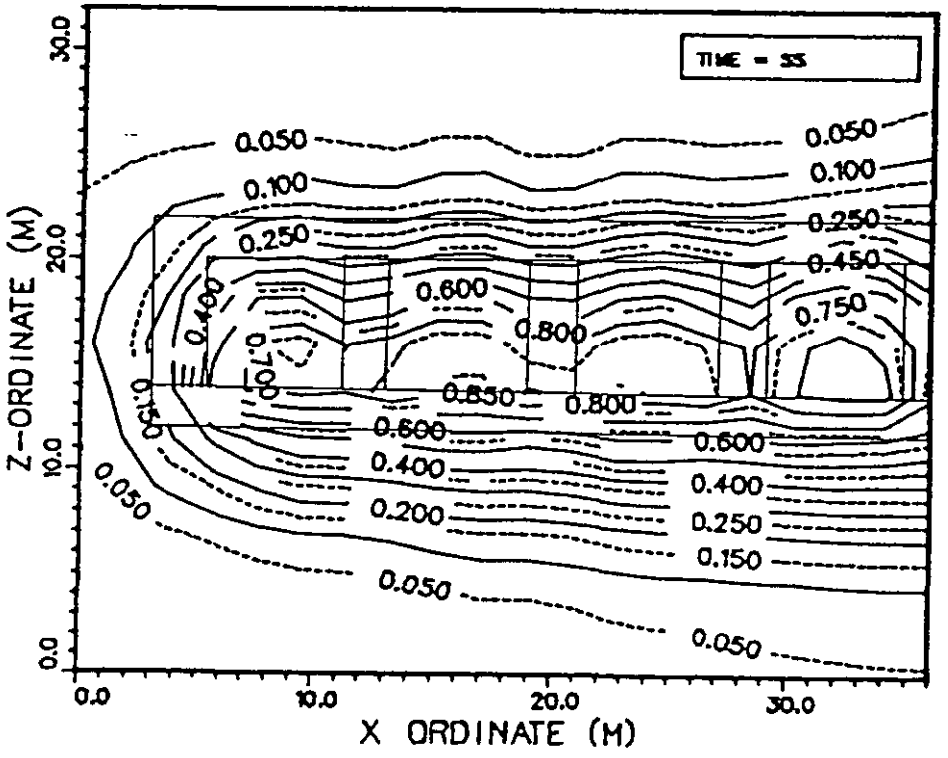

Figure 12. Normalized Salt Concentrations for the Reference Case.

4.1.2 Transient Calculation

Figures 13 (a), (b), and (c) indicate the concentration profiles for three different time periods of about 3 years, 7 years, and 12.5 years. The profile at 12.5 years clearly is essentially at steady state. By integrating the salt flowing out of the right-hand boundary and the salt that is still in the system, we found that most of the salt has not yet been leached out of the saltcrete. Thus the continuous cap system does not seem viable.

4.1.3 Total Saltcrete Flux - Revised Concentration Calculation

The concentrations shown in Figures 12 and 13 were calculated using an assumed dispersivity of 2 meters, uncorrected for saturation. This number is based on field experiements conducted at sites similar to SRP but in the saturated zone and under essentially horizontal flow conditions. Significantly lower values of dispersivity may apply at SRP in the zone of aeration. In particular, DuPont laboratory data suggest that the rate of diffusion within the monolith is many orders of magnitude smaller than simulated in Figure 12. These values cannot be simulated without a much finer mesh than that pictured in Figure 8. If we ignore diffusion and dispersion, an accurate estimate of salt convection to the water table can be obtained by examining the relative volumetric flux of water through the saltcrete monoliths, compared to water passing around them. 7.5% of the recharge actually passes through the monoliths, or 34.1×10^{-9} m^2/sec. This saltcrete flux number was calculated by numerically integrating the Darcy velocities along bottoms and sides of the monoliths. Assuming that this water emerges fully saturated with leachate at 209,100 mg/ℓ NO_3^-, then the average concentration reaching the water table at steady state is roughly:

$$0.075 \times 209{,}100 \text{ mg}/\ell = 15{,}700 \text{ mg}/\ell \ NO_3^-$$

This concentration can be compared to the much more conservative estimates of Figure 12, that account for convection and an overly large dispersion. Calculating the average volumetric concentration reaching the water table by accounting for flow Darcy flow rate in Figure 12, we get 29,200 mg/ℓ, or approximately twice that of convection alone. The actual concentration should

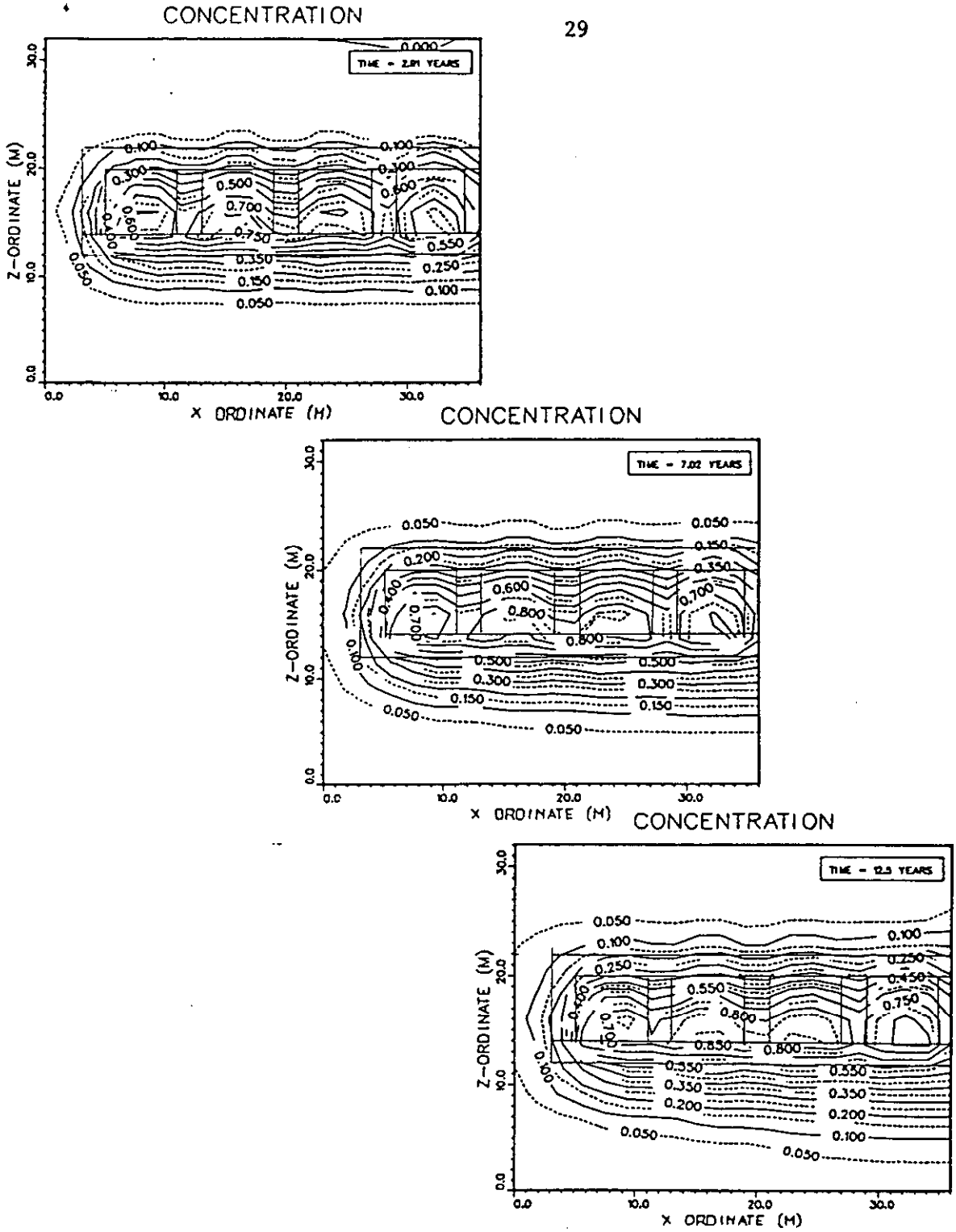

Figure 13. Transient Normalized Salt Concentration Profiles.

be much closer to the lower convection based value. Consequently, the convection calculation rather than the transport model was generally used to evaluate subsequent design options. In either case, the concentrations significantly exceed drinking water standards for nitrate.

4.1.4 Sensitivity to Soil Curves

The curves indicated by the dashed lines in Figure 3(a) (b) enclosed the primary uncertainty range for both host soil and backfill. We decided to investigate the sensitivity of the results to both ends of this uncertainty range. The curve set labeled (1) for both pressure head and relative permeability represents soils with apparently more sand content than the average. The curve set labeled (2) represents a clayey type soil. The results for these sets of curves are illustrated in two ways. First, the travel times to the right-hand-boundary for water particles placed at the bottom of each monolith were compared to the reference case. Second, integrated volumetric saltcrete flux out of each monolith were also compared. These results are given in Table 3 for the travel times and Table 4 for the integrated saltcrete fluxes. The effect of the sandy (1) type curve is to marginally decrease the flux through the monoliths. The maximum difference in integrated flux between the higher sand content case and the reference case is about 25% for monolith 1. The net integrated flux for all four monoliths differs by less than 10%. Travel times from the monoliths show a decrease of as much as 20%. The effect of the clayey (2) type curves is mixed. The maximum difference in integrated flux for a single monolith is less than 3% and the cumulative is only slightly more than 1%. Travel times are generally increased.

The calculated flux and travel times are relatively insensitive to assumptions about soil properties. Higher clay content does not significantly change the flux and actually reduces the travel time. Higher sand content conservatively leads to a decreased salt flux with a marginally higher travel time. These results do not change the conclusion that a continuous clay cap cannot meet the drinking water nitrate standard below the water table.

TABLE 2. TRAVEL TIME SENSITIVITY TO VARIATIONS IN CAPILLARY PRESSURE AND RELATIVE PERMEABILITY DATA

TRAVEL TIME (Years)

Particle	Unsaturated Property Curves (2)	Reference	(1)
A	24.6	28.9	26.4
B	26.6	29.4	37.8
C	17.3	18.3	26.1
D	32.5	38.1	38.8
E	27.7	31.5	31.5
F	15.0	16.0	20.0
G	29.0	34.0	30.7
H	24.1	29.4	25.1
I	12.4	13.2	16.0
J	25.4	30.7	24.9
K	20.5	25.1	20.0

STARTING LOCATIONS

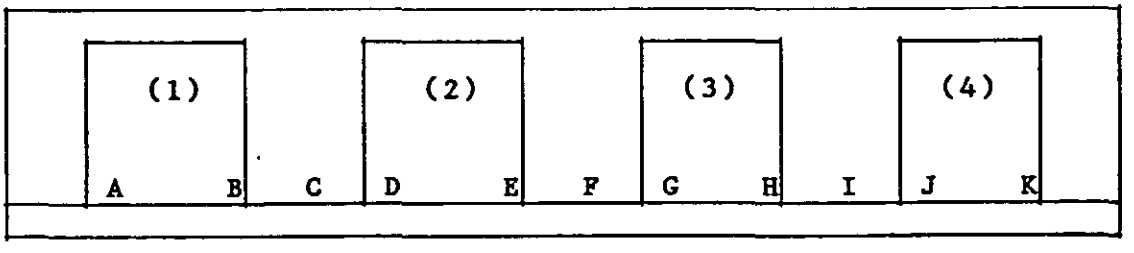

Table 4: INTEGRATED VOLUME EFFLUX FROM SALTCRETE FOR RANGE IN UNSATURATED PROPERTIES (m^3/sec/m), CONTINUOUS CAP

	Unsaturated Property Curves		
Monolith No.	Curve Set 1	Reference	Curve Set 2
1	6.63×10^{-9}	8.92×10^{-9}	9.02×10^{-9}
2	6.91×10^{-9}	8.02×10^{-9}	7.82×10^{-9}
3	8.32×10^{-9}	8.44×10^{-9}	8.29×10^{-9}
4	9.05×10^{-9}	8.73×10^{-9}	8.59×10^{-9}
Total	30.91×10^{-9}	34.11×10^{-9}	33.72×0^{-9}

4.2 GENERAL EVALUATION OF A DISCONTINUOUS CLAY CAP

The basic problem with continuous clay cap is that the infiltrating water must travel a large distance to pass around the waste form grid of saltcrete monoliths. This is illustrated most clearly in Figure 9. As a consequence water ponds on top, as shown in Figures 10 and 11, and as much as 20% of the total recharge passes through the monoliths. To reduce this flux through the monoliths additional area must be provided for the water to flow around them. This can be accomplished by deleting the cap and liner between the saltcrete monoliths, thus opening up a flow channel. This discontinuous cap design was evaluated next.

Three cases of the full saltcrete waste form grid were run to examine the sensitivity of a discontinuous clay cap to hydraulic conductivity and the importance of a liner. Subsequently symmetry was employed to examine just one saltcrete monolith, in order to investigate options for placing a clay lining around the waste form. These results are described in the following two subsections.

4.2.1 Original Design - Full Waste Grid

The original design investigated consisted of the same finite element mesh shown in Figure 8 but with a discontinuous clay cap. A low permeability clay cap, with and without liner, and a zero permeability clay cap were examined.

4.2.1.1 Low Permeability Clay Cap

In this simulation the unsaturated properties used for the soil and waste form were identical to those used in the reference case (saturated hydraulic conductivities of 10^{-6} cm/sec for saltcrete and 10^{-6} cm/sec for liner). The clay cap permeability was reduced to 10^{-9} cm/sec. The results are summarized in Table 5 in terms of integrated volumetric flow through the saltcrete monoliths and contrasted to the continuous clay cap case. Note that for the continuous cap the saltcrete flux is less than 30% of the reference case. Part of this reduction is due to the gaps between the monoliths, and part is due to the reduction of clay cap saturated hydraulic conductivity. The

Table 5: INTEGRATED VOLUME EFFLUX FROM SALTCRETE FOR RANGE IN CAP AND LINER PERMEABILITY (m^3/sec/m), DISCONTINUOUS CAP

Monolith No.	Continuous Cap 10^{-7} cm/sec	Discontinuous Cap 10^{-9} cm/sec Cap	Discontinuous Cap 0 Perm Cap	Discontinuous 10^{-9} cm/sec Cap & Liner
1	8.92×10^{-9}	1.97×10^{-9}	1.97×1^{-9}	1.08×10^{-9}
2	8.02×10^{-9}	2.45×10^{-9}	$2.45 \times ^{-9}$	1.20×10^{-9}
3	8.44×10^{-9}	2.61×10^{-9}	2.61×10^{-9}	1.28×10^{-9}
4	8.73×10^{-9}	2.68×10^{-9}	2.68×10^{-9}	1.31×10^{-9}
Total	34.1×10^{-9}	9.71×10^{-9}	9.71×10^{-9}	4.87×10^{-9}
Percent of Recharge	7.5	2.1	2.1	1.1
Nitrate Concentration (mg/ℓ)	15700	4400	4400	2300

nitrate concentrations shown are calculated by looking at convection only (see Section 4.1.3), neglecting diffusion and dispersion out of the monoliths. Streamlines for this case are shown in Figure 14.

4.2.1.2 Zero Permeability Clay Cap

As Table 5 indicates, the results for this case are identical to the low permeability clay cap. At 10^{-9} cm/sec the clay cap is essentially impervious.

4.2.1.3 Low Permeability Cap and Liner

Adding the liner reduces the saltcrete convective flux by an additional factor of two.

If one examines the concentrations in Figure 4, which result from the convective flux of water and salt through the waste form, the nitrate water quality standard would still not be met. Further design modifications were necessary.

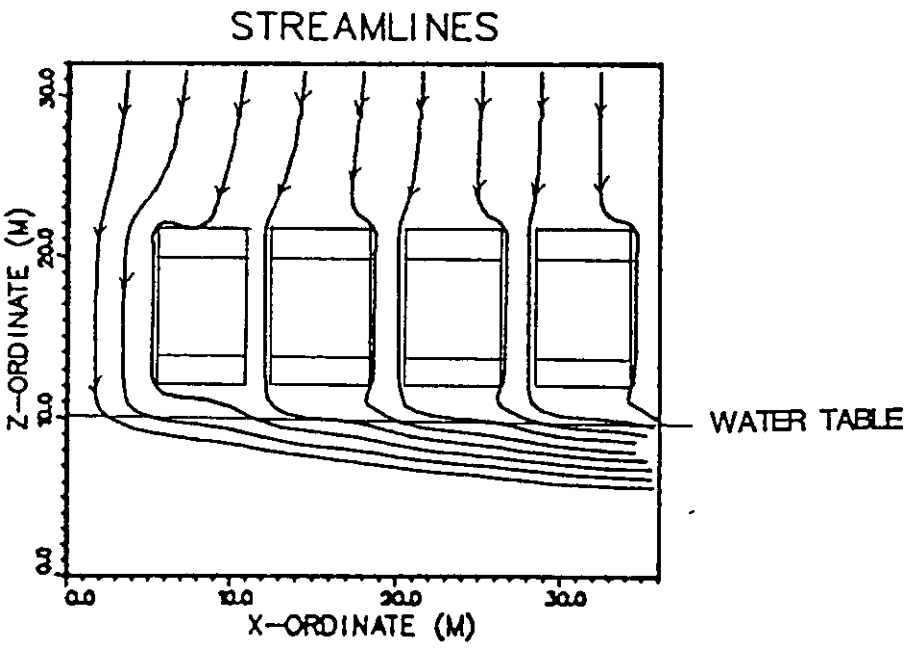

Figure 14. Streamlines for the Discontinuous Cap.

4.2.2 First Modified Designs - Single Monolith Calculations

To further reduce the saltcrete flux and nitrate concentrations, the design was modified. The waste form monoliths were separated from each other by greater distances and examined individualy. Four designs for individual monoliths were investigated. The first design was virtually identical to the low permeability clay cap case but with a lower saltcrete permeability 10^{-7} cm/sec. The remaining three designs have sloped sides. These designs, shown in Figure 1(c) - 1(f), include the following variations:

- a clay cap over the waste form (Cases 1 and 2);
- a clay umbrella extending somewhat beyond the waste form (Case 3); and
- a clay cap all around the waste form (Case 4).

In these cases the clay cap had a saturated hydraulic conductivity of 10^{-9} cm/sec and was 5 feet thick. The rectangular monolith was 20 feet tall, and 20 feet wide. The trapezoidal monoliths were of the same height, 10 feet wide at the bottom and 30 feet wide at the top. The monoliths were spaced 50 feet apart, center to-center, with 15 feet of backfill over them. Between the monoliths host soil was kept in place. The host soil saturated conductivity was decreased to 10^{-4} cm/sec. The water table was located 15 meters below ground level (compared to 22 m in the reference case) or 3 m below the monolith. At the water table a constant zero pressure boundary was applied. No flux boundaries of symmetry were taken at the left and right. At the top 40 cm/yr of infiltration was applied.

The results for these cases are illustrated in Tables 6 and 7. These tables summarize the flow through the waste form monolith and the nitrate concentrations which would result from the flow and from molecular diffusion (assuming the duPont laboratory determined diffusion flux of 10^{-5} g/cm^2/day for total saltcrete dissolution). Table 7 indicates that the last design (enclosed in clay) could satisfy the nitrate standard considering both convection and diffusion. The two independent numbers in Table 5 for convection (flow through) and diffusion are average values and were calculated assuming the nitrate exiting the monolith perfectly mixed with the total infiltration at the surface.

Table 6: VOLUME EFFLUX FROM SINGLE SALTCRETE MONOLITH

CASE	FIGURE	MONOLITH SHAPE	CAP	STEADY STATE FLOW THROUGH MONOLITH (m^3/sec/m)	PERCENT OF TOTAL RECHARGE
1	1c	Rectangular	top	8.5×10^{-11}	.073
2	1d	Trapezoidal	top	3.1×10^{-11}	.023
3	1e	Trapezoidal	overhang	2.6×10^{-11}	.019
4	1f	Trapezoidal	liner	9.3×10^{-12}	0.007

TABLE 7: NITRATE CONCENTRATIONS IN RECHARGE TO GROUND WATER DUE TO:

CASE	CONVECTION	DIFFUSION*
1	153 mg/l	5.4 mg/l
2	48	4.9
3	40	4.9
4	14	4.9
STANDARD	44	

*Note: Assumes leach rate of 1×10^{-5} g/cm^2/day of saltcrete over entire area.

Referring to Figure 1(c) - 1(f) and Table 6, the following observations can be made. Changing the cross-sectional shape of the capped saltcrete monolith from a rectangle to a trapezoid reduces the flow through the monolith. The greatest source of water for this flow is water that infiltrates downward from the surface, that flows around the clay cap and then in through the side of the monolith, as illustrated in Figure 15 for the rectangular monolith. Because the side of the trapezoidal monolith slopes away from the cap, less water penetrates the side and thus the flow through the monolith is reduced. This observation remains true only so long as the area between adjacent monoliths remains fairly large, in order to avoid significant ponding on top. The relevant distance seems to be 1/2 of the distance from monolith center to center, although further design studies would be necessary to optimize this design parameter. Extending the cap beyond the edge of the monolith, as shown in Figure 1(e), further reduces the rate of flow through the monolith, although only marginally. Again the extension must be limited in order to leave a large open area between monoliths. Finally, surrounding the monolith with a liner, as in Figure 1(f), further reduces the saltcrete flow. However the construction cost of this last alternative may significantly outweight the reduction obtained.

Complete transport calculations were also done for some of the single monolith cases. For Case 1, the rectangular monolith geometry, the integrated concentration exiting the calculational system was just over 190 mg/ℓ. The sum from Table 7 is just less than 160 mg/ℓ. Thus the two calculations are in fairly good agreement.

Based upon these calculations, the design involving sloped sides and clay enclosing a saltcrete monolith could meet the nitrate standard. The net concentration of nitrate at the water table which came from flow through the saltcrete was about 14 mg/l. Diffusion, for a leach rate of 1×10^{-5} $g/cm^2/day$ of saltcrete, adds about 5 mg/l. All of these results are based upon the best estimate soil properties representative of data at the site. Factors of about two difference, though, can be calculated from reasonable changes in soil properties. Even so the standard of 44 mg/l could be met with this design. The other two sloping side designs with clay only over the top would come close to meeting the standard.

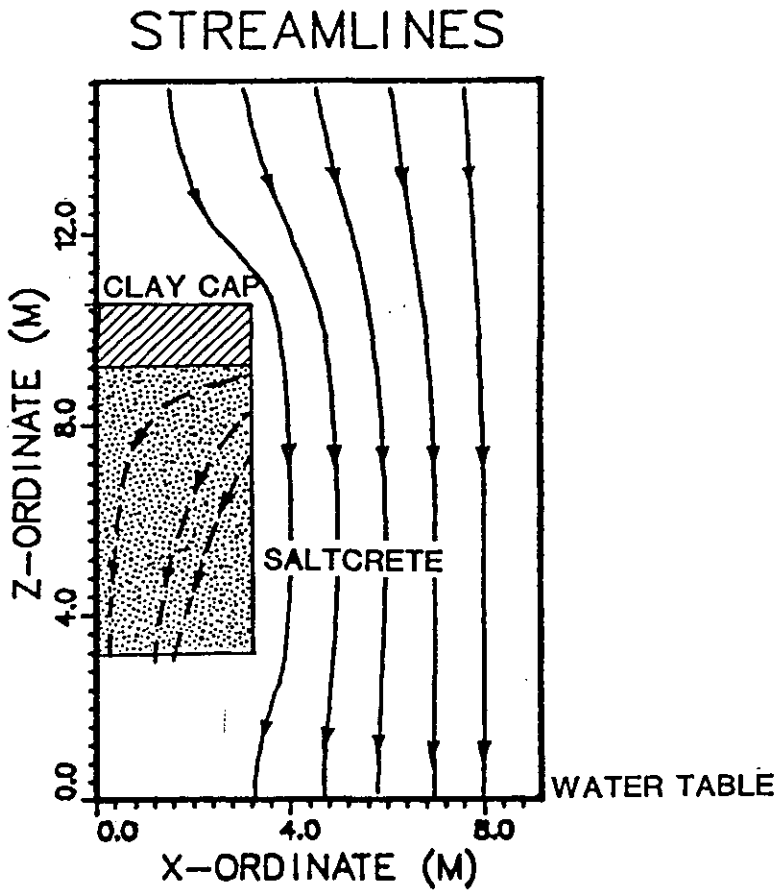

Figure 15. Streamlines for a single rectangular monolith. The solid lines are streamlines originating at the ground surface. The dashed lines are streamlines for water entering the saltcrete monolith. The origin for this water is at the ground surface where $x \cong 0$, that is right above the centerline of the monolith.

It will be extremely difficult to install a clay cap with 10^{-9} cm/sec hydraulic conductivity. To test this assumption Case 4 was also run with 10^{-8} cm/sec for clay. This gave a convective contribution of 70 mg/ℓ and thus could not satisfy the standard. Additional studies were required, to find an acceptable design with a clay cap conductivity of only 10^{-8} cm/sec.

4.3 DETAILED EVALUATION OF DESIGNS FOR A SINGLE SALTCRETE MONOLITH

These design studies have demonstrated the need to treat each monolith individually, by providing ample area between monoliths for infiltration to reach the water table without passing through the monoliths. Of the other design features evaluated, those worth emphasizing are:

- the use of a cap and a cap overhang to reduce leaching potential,
- the use of sloped trench sides to construct trapezoidal shaped monoliths, thus reducing construction costs and leaching potential, and
- the minor reduction of leaching potential caused by lining the trench, an expensive design feature that may not be justified by this minor reduction.

These considerations were incorporated into a new set of designs for the saltcrete monoliths. Liners were not used because of their cost and minor impact. To reduce the potential for water to "pond" on the top of the cap over the monolith, the cap was given slopes of 15% and 50%. Caps composed of clay were assigned a saturated hydraulic conductivity of 10^{-8} cm/sec, an order of magnitude higher than the value used in the tests described in Section 4.2. Gravel caps were also investigated, using the so-called "wick effect" to prevent moisture penetration into the cap and underlying saltcrete (see, e.g., Frind et al, 1976; Lindsay, et al, 1980; Rancon, 1980). Finally, further laboratory studies at SRP demonstrated that a revised mixture of material results in a saltcrete with a saturated hydraulic conductivity of only 5×10^{-10} cm/sec, orders of magnitude lower than that given by the original mixture. The monoliths were assumed to be composed of this material. With the exception of a single sensitivity analysis simulation, the saltcrete unsaturated properties were not changed.

In cross-section the trapezoidal monolith was 25 feet tall, 40.5 feet wide at the top, and 15.5 feet wide at the bottom. The sides sloped steeply at 1:2. The top of the monolith was situated 16.4 feet below the ground surface. When installed with a 15% slope, the cap was 2 feet thick, and set on 3.4 feet of fill above the monolith at its centerline. The fill decreased in thickness uniformly until at the edge of the monolith it is only 4.5 inches thick. Consequently there was 11 feet of backfill over the cap at the centerline and 14.4 feet at the edge. With a 50% slope the 2 foot thick cap sat on 11.4 feet of fill at the centerline, and 15 inches of fill above the edge of the monolith, leaving 3 feet and 15 feet of backfill over the cap. Both caps extended 2.5 feet beyond the edge of the monolith. The fill material between the cap and the saltcrete was designed to have the same properties as the backfill. The monoliths were spaced 42.25 feet apart, center to center. The host soil, at $K=10^{-3}$ cm/sec, filled the area between the monoliths. Note that this value is the same as used in the Reference Case, but an order of magnitude higher than the value used in Section 4.2.

40 cm/year of infiltration was applied to the top of a single monolith model. No-flow boundaries of symmetry were applied to the left and right. At the bottom, 16 meters below ground surface, a water table constant pressure boundary condition was prescribed. The water flow through the saltcrete was calculated and compared to the total infiltration. Typical total head, pressure head, saturation and velocity plots are given in Figure 16. The results presented in terms of percent infiltration are presented in Table 8 for all of the designs tested. Once again, assuming a fully saturated saltcrete leachate, these numbers were multiplied by 209,100 mg/ℓ to yield estimated average concentrations of NO_3^- reaching the water table by convection, as also shown in Table 8.

4.3.1 Clay Cap and Low Conductivity Saltcrete

Comparing cases 1 and 2 leads to the conclusion that using the new saltcrete mixture reduces the saltcrete flux and nitrate concentration to 0.1% of its fomer value. These two cases avoid the use of a cap. With the old saltcrete mixture the estimated nitrate concentration is 1820 mg/ℓ, much higher than permissible limits. Using the new mixture the estimated NO_3^-

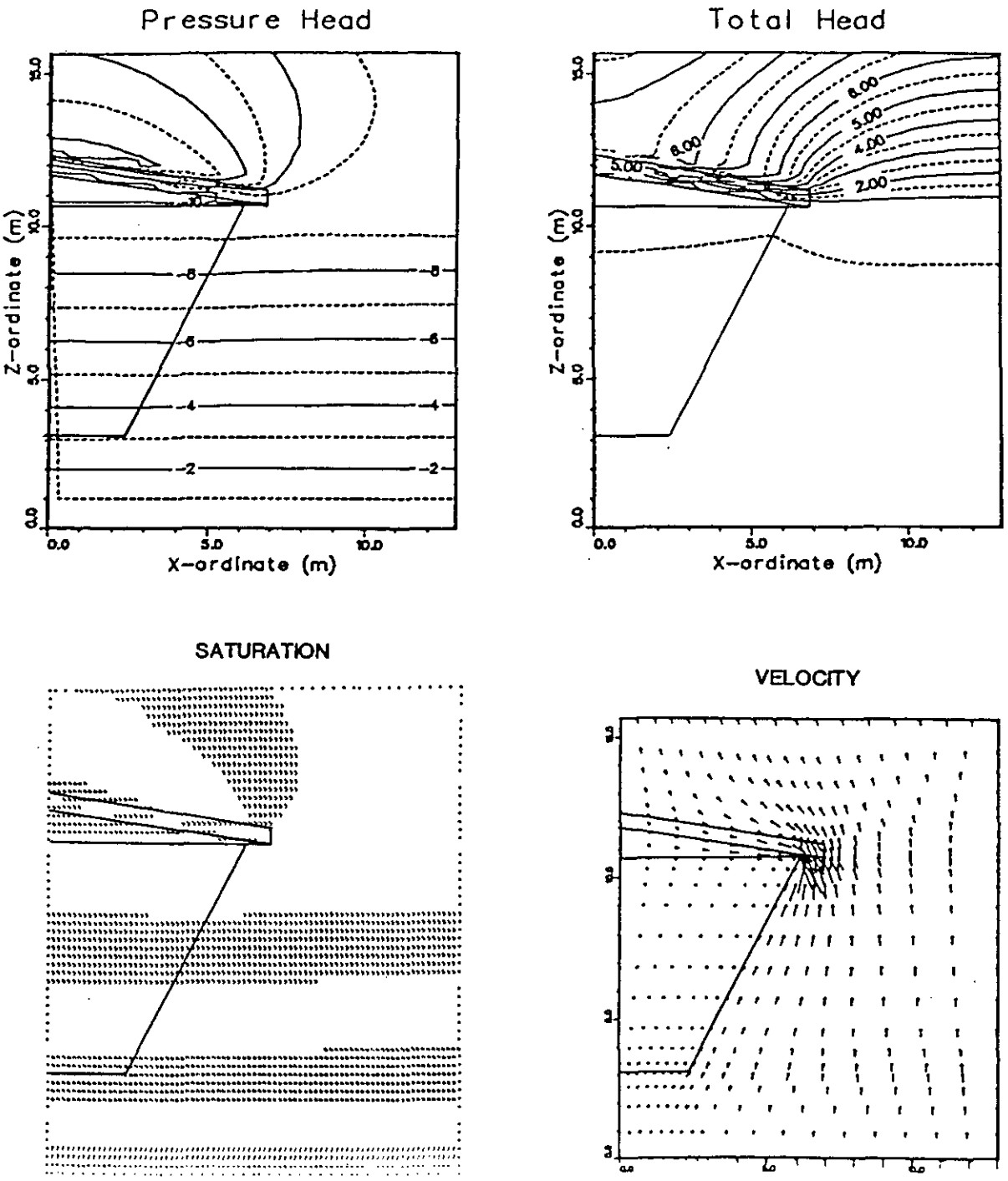

Figure 16. Total Head, Pressure Head, Saturation and Velocity for a Single Monolith Under a Clay Cap: Modified Saltcrete Mixture.

TABLE 8. VOLUME EFFLUX FROM SINGLE SALTCRETE MONOLITH AND NITRATE CONCENTRATIONS IN RECHARGE TO GROUNDWATER

Case	Saltcrete K (cm/sec)	Cap Type	Cap K (cm/sec)	Cap Slope %	Percent of Total Recharge	Nitrate Concentrations (mg/ℓ)
1	10^{-7}	None	NA*	NA*	0.87	1819
2	$5x10^{-10}$	None	NA	NA	$9x10^{-4}$	1.9
3	10^{-7}	Clay	10^{-8}	15	$4.3x10^{-3}$	9.1
4	$5x10^{-10}$	Clay	10^{-8}	15	$4.5x10^{-5}$	0.1
5	$5x10^{-10}$	Clay	10^{-8}	15	$8.4x10^{-5}$	0.2
6	$5x10^{-10}$	Clay	0	15	$3.4x10^{-5}$	0.1
7	$5x10^{-10}$	Clay	0	50	$3.3x10^{-5}$	0.1
8	$5x10^{-10}$	Gravel	10	50	$3.4x10^{-5}$	0.1
9	$5x10^{-10}$	Pseudo-Gravel	10	50	$5.7x10^{-4}$	1.2

* NA = not applicable

concentration is only 1.9 mg/ℓ, which is well within the drinking water standard of 44 mg/ℓ. Although the new saltcrete mixture alone results in a design capable of reducing leaching potential to acceptable levels, other redundant barriers to leaching were also evaluated. Comparing cases 1 and 3 shows that adding a clay cap with a 15% slope, to cover a saltcrete monolith that uses the old mixture, reduces saltcrete flux to 0.5% of its former value.

In case 4, both the new mixture and the 15% cap were used to obtain a reduction of saltcrete flux of 0.005% from case 1. The estimated nitrate concentration is only 0.1 mg/ℓ. The total head, pressure head and saturation plots for this case are shown in Figure 16. These plots demonstrate that the infiltrating water runs around the cap and the monolith to recharge the water table directly. Only 0.000045 percent of the infiltration ever enters the monolith. consequently, this design virtually prohibits any significant buildup of leachate by convection of water through the monolith. Even failure of the cap, or deterioration of the saltcrete integrety, alone still results in nitrate concentrations of less than 10 mg/ℓ. This design is conservatively redundant.

To check the dependence of these results on the assumed unsaturated properties of the saltcrete, the clayey soil type curves (2) from Figure 3 were used to represent the saltcrete. Shown as Case 5 in Table 8 the saltcrete flux doubled, but was still so small that the nitrate concentration was less than 0.2 mg/ℓ. The clayey curves result in a higher water saturation in the monolith, and thus a larger flux and concentration.

In Case 6, the saturated hydraulic conductivity of the cap was set to zero. Comparing to Case 4 shows that even at a saturated conductivity of 10^{-8} cm/sec the clay cap was virtually impervious. The slope of the impervious cap was increased from 15% to 50% in Case 7. This increase of slope has no significant impact for these steady state conditions. Under transient conditions, with higher but temporary infiltration rates, the large slope may prove to be a more significant design feature (Frind et al, 1976).

4.3.2 Gravel Cap and the Wick Effect

Using gravel to construct the cap sloping at 50% gives the results shown for Case 8. By comparing to Case 7 it is apparent that the gravel is almost impervious. The gravel properties were taken for a fairly uniform "pea sized" gravel. The properties included a saturated hydraulic conductivity of 10 cm/sec, and pore pressure and relatively permeability curves, respectively, given by:

$$p_c = p_b \, S_e^{-1/8}; \; p_b = (0.5 \text{ cm}) \, \rho g$$

$$k_r = S_e^{13/4}$$

where:

S_e = $\left(\frac{S_w - S_r}{1 - S_r}\right)$ = effective water saturation

S_r = residual irreducible water saturation = 0.02 for this gravel

$p_b/\rho g$ = capillary rise = 0.5 cm, ℓ, for this gravel

These curves are based on a capillary tube model of a porous media (Wilson and Gelher, 1974), with a pore size distribution described by the incomplete Beta function, $B(p_c/p_b; a+2, b)$ where for a uniform gravel a=5, b=0.

Using a gravel layer in this manner results in what is usually called the "wick effect" (Rancon, 1980). Although gravel has a higher saturated hydraulic conductivity than clay or the host soil, it is not saturated in this application. Its large pore size prevents entry of water because of capillary effects. The fine grained backfill above the gravel acts like a wick to conduct the water around the gravel, and thus around the saltcrete. Total head, pressure head, and saturation plots for this case are given in Figure 17. As indicated in Table 8 the estimated nitrate concentration is only 0.1 mg/ℓ.

To examine the dependence of this phenomenon on capillary effects the simulation was repeated with a gravel having the capillary properties of the other soils (a physical impossibility, a computer possibility). The result for this pseudo-gravel is shown as Case 9 in Table 8. The nitrate

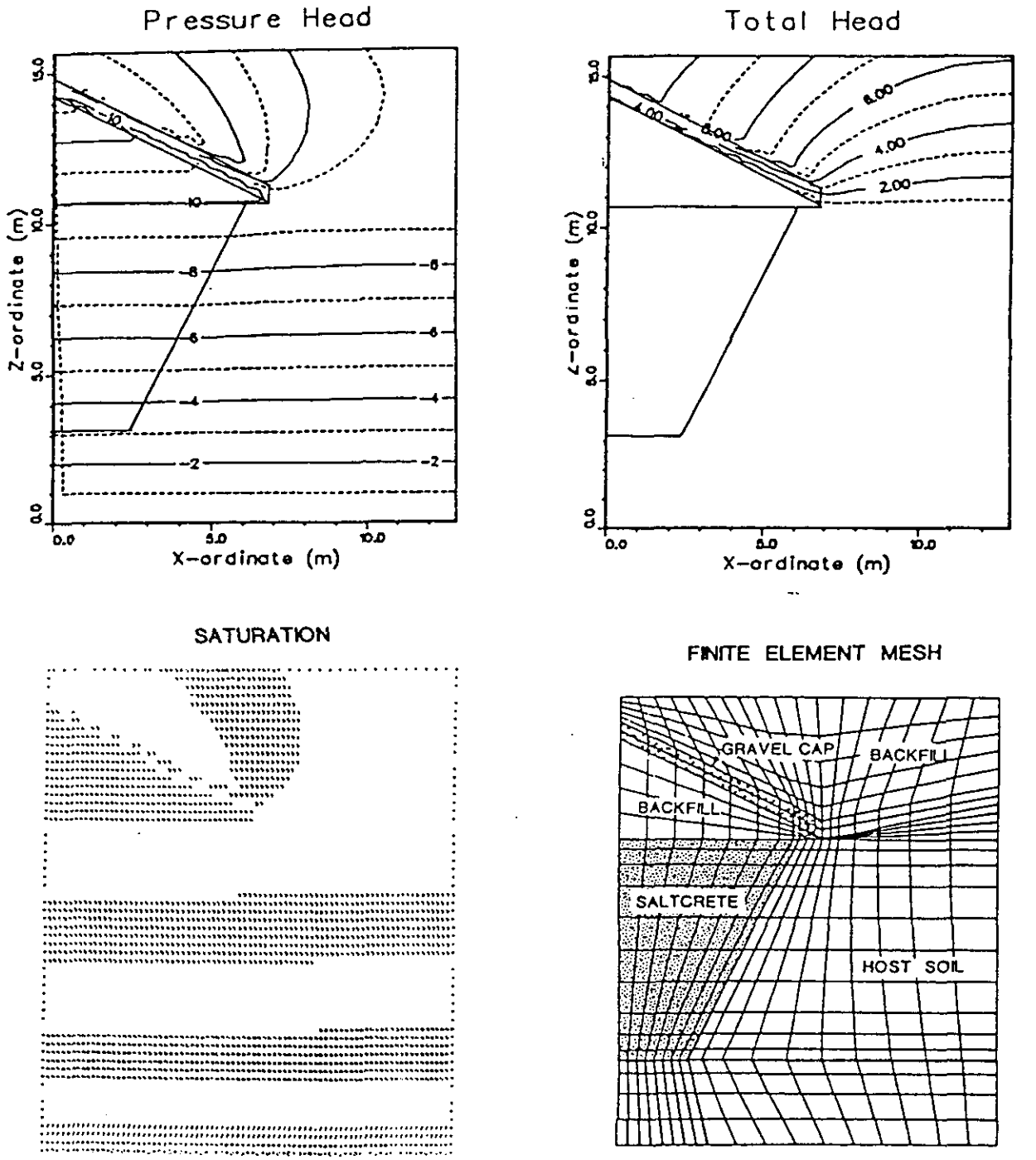

Figure 17. Total Head, Pressure Head and Saturation for a Single Monolith Under a Gravel Cap: Modified Saltcrete Mixture. The finite element mesh for the 50% sloping cap is also shown.

concentration entering the water table jumps to 1.3 mg/ℓ, a seventeen fold increase. So it is the capillary effects, not the saturated conductivity that creates a barrier. Another interesting observation arises after comparing Case 9 to Case 2. Placing a zone of high saturated conductivity of this pseudo-gravel over the monolith actually decreases water flow through the saltcrete, even though the unsaturated properties are the same in both cases. The high permeability zone attracts infiltration from almost 60% of the ground surface, then directs it around the monolith by discharging this water at the lower end of the pseudo-gravel zone, some 2.5 feet to the side of thw monolith. The pseudo-gravel acts something like a drain. If, under transient conditions, the real gravel becomes saturated it is possible that it will demonstrate similar behavior. Transient simulations will be necessary to verify this hypothesis.

5 CONCLUSIONS

A continuous clay cap over a number of saltcrete waste forms will result in nitrate leaching to the water table, with cncentrations greatly exceeding drinking water standards. To reduce this flux of NO_3^-, the area between the waste form monoliths must be open to vertical flow, so that water has a low resistance path to follow that avoids the saltcrete. To accomplish this the cap and liner must be deleted between the monoliths. The monoliths should be spaced such that they occupy no more than 50% of the area available for groundwater recharge.

Clay caps will significantly reduce the rate of nitrate leaching by reducing the water flow through the monoliths. Placing a slope on the cap and giving it an overhang improve the design. However, the slope should not be so steep as to prohibit sufficient soil backfill above the cap, say at least 3 feet, in order to prevent soil saturation during transient infiltration events. Similarily, the overhang should be limited in order to avoid reducing the size of the flow zone between monoliths.

Using a sloped side for a trapezoidal monolith is probably a good construction practice and has the additional benefit of reducing flux through a capped monolith, provided the flow zone area between monoliths is preserved.

Using gravel in the cap leads to the so-called "wick effect", and provides a barrier to steady water flow through the gravel that is as effective as a clay cap. However, it may be subject to failure during transient infiltration events and its long term integrity has not been demonstrated.

Replacing the original saltcrete mixture with a low hydraulic conductivity mixture has a significant influence on the rate of water flow through the monolith. As long as the integrity of the monolith is preserved, this single feature is adequate to reduce convective leaching to negligible levels. Then additional barriers, such as a clay cap, become redundant.

6 RECOMMENDATIONS

There are two areas that need additional evaluation. Transient analyses should be made to verify that the design selected from these steady-state studies also works when infiltration varies in time. Hypothetical time histories for the infiltration could be used, or these analyses could be coupled with the simulations proposed in our second recommendation.

We believe it would be advisable to compare the model used here through a field validation. As we understand it, there is a field test of a saltcrete waste form which has been emplaced in the soil for some period. If soil properties are available from this area, we believe two sets of computer runs would be advisable. These would include:

(1) calculation using the measured soil properties and comparing the results to the observed field test;

(2) calculation using the field geometry but using soil properties from this present study to determine the difference in predicted results from using actual soil properties at the validation site. This comparison would provide sensitivity results.

7 REFERENCES

Duguid, J.O., and M. Reeves, 1976. "Material Transport Through Porous Media: A Finite Element Galerkin Model", ORNL-4928, Oak Ridge National Laboratory, Oak Ridge TN.

Frind, E.O., Gillham, R.W. and J. F. Pickens, 1976. "Application of Unsaturated Flow Properties in the Design of Geologic Environments for Radioactive Waste Storage Facilities", Proceedings of Finite Elements in Water Resources, Pen Tech Press, London.

Gruber, P., 1981. "A Hydrologic Study of the Unsaturated Zone Adjacent to a Radioactive-Waste Disposal Site at the Savannah River Plant, Aiken, SC., M. S. Thesis, University of Georgia.

Hillel, D., 1977. Computer Simulation of Soil Water Dynamics, International Development Research Center, Ottawa, Canada.

Lindsay, L.E., Gillham, R.W. and E.O. Frind, 1980. "Studies of Engineered Geologic Environments for Radioactive Waste Storage", TR-27, Atomic Energy of Canada, Limited.

Racon, D., 1980. "Application de la Technique des Barriers Capillaries aux Stockages en Transchees", Proceedings of Underground Storage of Radioactive Wastes, Vol. 1, SM-243/71, IAEA, Vienna.

Reeves, M. and J. O. Duguid, 1975. "Water Movement Through Saturated-Unsaturated Porous Media: A Finite Element of Galerkin Model:, ORNL-4927, Oak Ridge National Laboratory, Oak Ridge, TN.

Root, R.W., 1980. "Results of Laboratory Tests on Undisturbed Subsurface Samples from F and H Areas", Memorandum to I. W. Marine, Waste Disposal Technology Division, SRP, E.I. duPont de Nemours & Company, Aiken, S.C.

Wilson, J.L. and L.W. Gelhar, 1974. "Dispersive Mixing in a Partially Saturated Porous Media:, TR 191, Ralph M. Parsons Laboratory for Water Resources and Hydrodynamics, Mass. Inst. of Tech., Cambridge.

Yeh, G.T. and D. Ward, 1980. "FEMWATER: A Finite-Element Model of Water Flow Through Saturated-Unsaturated Porous Media", ORNL-5567; FEMWASTE: A Finite Element Model of Water Transport Through Porous Saturated-Unsaturated Media:, ORNL-5601; Oak Ridge National Laborabory, Oak Ridge, TN.